AFFDL-TR-70-125

EFFECT OF FIBER ORIENTATION ON INITIAL POSTBUCKLING BEHAVIOR AND IMPERFECTION SENSITIVITY OF COMPOSITE CYLINDRICAL SHELLS

N. S. KHOT

V. B. VENKAYYA

TECHNICAL REPORT AFFDL-TR-70-125

DECEMBER 1970

AIR FORCE FLIGHT DYNAMICS LABORATORY
AIR FORCE SYSTEMS COMMAND
WRIGHT-PATTERSON AIR FORCE BASE, OHIO

NOTICE

When Government drawings, specifications, or other data are used for any purpose other than in connection with a definitely related Government procurement operation, the United States Government thereby incurs no responsibility nor any obligation whatsoever; and the fact that the government may have formulated, furnished, or in any way supplied the said drawings, specifications, or other data, is not to be regarded by implication or otherwise as in any manner licensing the holder or any other person or corporation, or conveying any rights or permission to manufacture, use, or sell any patented invention that may in any way be related thereto.

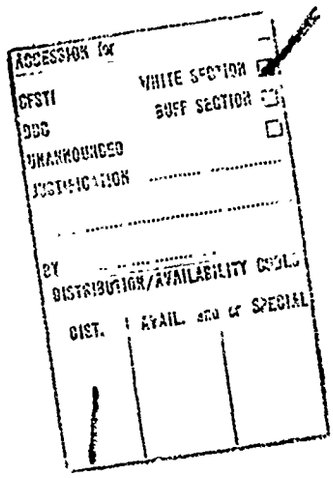

Copies of this report should not be returned unless return is required by security considerations, contractual obligations, or notice on a specific document.

400 - January 1971 - CO305 - 22-71-364

AFFDL-TR-70-125

EFFECT OF FIBER ORIENTATION ON INITIAL POSTBUCKLING BEHAVIOR AND IMPERFECTION SENSITIVITY OF COMPOSITE CYLINDRICAL SHELLS

N. S. KHOT

V. B. VENKAYYA

ABSTRACT

Koiter's approach is used to formulate the influence of fiber orientation on the behavior of the cylindrical shell in the initial postbuckling region. Results are presented for three-layer composite cylindrical shells of either glass-epoxy or boron-epoxy subjected to uniform axial compressive load. The results show that the initial postbuckling coefficient that characterizes the extent of imperfection sensitivity of a structure is greater for the glass-epoxy shells than for the boron-epoxy shells. For the glass-epoxy cylinders the slope of the load vs. end-shortening curve in the initial postbuckling region is found to have high negative value, which is not significantly affected by the change in fiber orientation. This suggests that the buckling of a nearly perfect glass-epoxy cylinder under prescribed end-shortening will be catastrophic, regardless of fiber orientation. However, for the boron-epoxy cylinders the negative slope varies with the change in fiber orientation, and whether the failure will be catastrophic or not will depend on the fiber orientation.

FOREWORD

This report is prepared as a part of in-house effort under Project No. 1467, "Structural Analysis Methods," Task 146703, "Structural Shell Analysis." The work was carried out in the Structural Synthesis Group of the Solid Mechanics Branch, Structures Division of the Air Force Flight Dynamics Laboratory, Air Force Systems Command, Wright-Patterson AFB, Ohio. Mr. Francis J. Janik, Jr. (FBR) was the Project Engineer administering Project 1467.

This report covers the work conducted during the period December 1969 to May 1970. The report was submitted by the authors in June 1970.

This technical report has been reviewed and is approved.

FRANCIS J. JANIK, JR.
Chief, Solid Mechanics Branch
Structures Division
Air Force Flight Dynamics Laboratory

TABLE OF CONTENTS

ILLUSTRATIONS

SYMBOLS

$a_{ij} = [a]$	in-plane compliance matrix
a	initial postbuckling coefficient; see Eq 11
b	initial postbuckling coefficient; see Eq 11
$d_{ij} = [d]$	compliance coupling matrix
$d^*_{ij} = [d^*]$	modified bending stiffness matrix
E_{11}, E_{12}, E_{22}	elastic constants
e_{avg}	average end-shortening; see Eq 44
$e_{c\ell}$	pre-buckling average end-shortening at buckling load
e	end-shortening
$\overset{\circ}{e}$	prebuckling end-shortening; see Eq 46
$\overset{(1)}{e}, \overset{(2)}{e}$	see Eq 46
F	modified Airy stress function; see Eq 9
$\overset{\circ}{F}$	modified prebuckling Airy stress function; see Eq 17
$\tilde{F}$	Air stress function
$\overset{(1)}{F}, \overset{(2)}{F}, \overset{(3)}{F}$	see Eq 17
h	amplitude of radial deflection parameter; see Eq 24

SYMBOLS (CONTD)

$\bar{h}$	amplitude of radial initial displacement; see Eq 54
$\tilde{k}_x, \tilde{k}_y, \tilde{k}_{xy}$	changes of curvature and torsion
K	see Eq 14 and 53
ℓ	$L/(4R^2 d_{11}^* a_{22})^{1/4}$
L	length of circular cylinder
L_i	linear differential operator
m	number of axial half-wavelengths
$\tilde{M}_x, \tilde{M}_y, \tilde{M}_{xy}$	resultant moments
M	$\frac{m\pi}{\ell} + \frac{n}{r}\tau$
M_i	$\frac{i\pi}{\ell} + \frac{2n\tau}{r}$
n	number of circumferential waves
N	n/r
$\overset{\bullet}{N}_x$	buckling load, lbs/in
N_x, N_y, N_{xy}	modified resultant membrane stresses; see Eq 9
$\bar{N}_x$	buckling load parameter
$\tilde{N}_x, \tilde{N}_y, \tilde{N}_{xy}$	resultant membrane stresses in shell

SYMBOLS (CONTD)

$\mathring{N}_x, \mathring{N}_y, \mathring{N}_{xy}$	prebuckling modified resultant stresses
$\mathring{\tilde{N}}_x, \mathring{\tilde{N}}_y, \mathring{\tilde{N}}_{xy}$	prebuckling resultant stresses
p	modified external pressure
$\tilde{p}$	external pressure
P	$\frac{m\pi}{\ell} - \frac{n\tau}{r}$
P_i	$\frac{i\pi}{\ell} - \frac{n\tau}{r}$
R	radius of the cylinder's reference surface
r	$R / (4R^2 d_{22}^* a_{22})^{1/4}$
t	thickness of the shell
$T_1, T_2, \cdots$	defined by Eq 29 and 30
$\tilde{U}$	axial displacement
U	$\tilde{U} / (4R^2 d_{11}^* a_{22})^{1/4}$
$\tilde{V}$	circumferential displacement
V	$\tilde{V} / (4R^2 d_{22}^* a_{22})^{1/4}$
$\tilde{W}$	radial displacement
W	modified radial displacement $\tilde{W} \sqrt{a_{22} d_{22}^*}$
$\overline{W}$	initial displacement of unloaded shell (imperfection)
$W^{(1)}, W^{(2)}, W^{(3)}$	see Eq 17

SYMBOLS (CONTD)

$\overline{W}^*$	$\bar{h}/h$
$\tilde{x}$	axial coordinate
x	$\tilde{x}/(4R^2\, d_{11}^*\, a_{22})^{1/4}$
$\tilde{y}$	circumferential coordinate
y	$\tilde{y}/(4R^2\, d_{22}^*\, a_{22})^{1/4}$
$\tilde{z}$	radial coordinate
S_1, S_2	defined by Eq 42 and 43
$\alpha_i, \beta_i, \gamma_i, \delta_i$	defined by Eq 34, 36, and 37
$\alpha, \beta, \gamma, \kappa, \xi\ \bar{\lambda}$ $\psi, \rho, \nu, \eta, \zeta, \phi$	defined by Eq 9
ϵ	perturbation coefficient (here it is the ratio of buckling displacement amplitude to the thickness of the shell)
λ	scalar load parameter
λ_c	classical value of scalar load parameter which is taken to be unity
λ_s	maximum value of scalar load parameter for an imperfect structure
τ	see Eq 24
$[\tilde{\epsilon}] = \tilde{\epsilon}_x, \tilde{\epsilon}_y, \tilde{\epsilon}_{xy}$	strain at reference surface
θ	fiber orientation; see Figure 1
$\tilde{\theta}$	angle of initial slope of postbuckling load vs end-shortening curves; see Figure 2, $\tan^{-1}\left(\frac{K}{K+1}\right)$
ρ^*	λ_s / λ_c

SECTION I

INTRODUCTION

The use of advanced fiber-reinforced composite structural elements in aerospace industry has been steadily increasing because of their high strength-to-weight ratios. Considerable effort has been expended in recent years to investigate the behavior of composite structures and their application to aerospace structures. This report presents results of an investigation of the initial postbuckling behavior and imperfection sensitivity of composite cylindrical shells, a common structural element of aerospace craft. It is well known that the classical buckling load obtained by using linear theory is generally incapable of predicting the actual buckling load. The discrepancy between the actual buckling load and the analytical one is attributed to the departure of the actual shell from the perfect geometry of the shell assumed for linear analysis. In general, imperfections in the initial geometry are not deterministic, and even if they were it would be difficult to incorporate them into an exact mathematical analysis. However, it is possible to make qualitative study of their effect on buckling load by making certain simplifying assumptions. The behavior of the perfect structure in the initial postbuckling region can also be used to predict the behavior of the actual shell.

The analytical approach selected for this investigation is based on Koiter's theory (References 1, 2, and 3). Using the principle of potential energy Koiter has established a technique to deal with the initial postbuckling behavior and the imperfection sensitivity of the structure. Koiter's theory starting from the principle of virtual work was further developed and reformulated by Budiansky and Hutchinson (References 4 and 5). The extensive application of Koiter's theory to shell-type structures can be found in References 6 through 22. Application of Koiter's theory to frames and trusses can be found in other references.

Each lamina of a composite shell is orthotropic with reference to its material axis. However, in the case of more than one lamina, if the material axis in each lamina do not coincide with the geometric reference coordinates of the structure, the composite shell can be considered as an anisotropic shell. The general theory of anisotropic shells has been developed by Ambartsumyan (Reference 23). Dong et al (Reference 24) and Cheng and Ho (Reference 25) have

presented a linear theory to investigate the buckling behavior of anisotropic cylindrical shells. Holston et al (Reference 26) and Tasi et al (Reference 27) have investigated the buckling strength of filament wound cylinders utilizing the linear theory in Reference 25. The postbuckling behavior and the influence of initial geometric deviations have been investigated in References 28 through 30 by applying nonlinear theory. In these references the principle of stationary potential energy is applied, and the resulting nonlinear algebraic equations are solved by the Newton-Raphson iterative technique.

The numerical results presented in this report are for three-layer cylindrical shells of either glass-epoxy or boron-epoxy composites subjected to axial compression. Because of the large number of parameters involved in this analysis, the only variable is the fiber orientation in each layer while the geometric properties of the shell remain fixed. The results presented in Section III reveal the influence of fiber orientation and material properties on the classical buckling load, initial postbuckling behavior, and the imperfection sensitivity of the cylindrical shell.

SECTION II

ANALYTICAL FORMULATION

1. STRESS-STRAIN RELATIONS

The constitutive equations for the composite laminated shell wall are given by

$$\left[\tilde{\epsilon}\right] = \left[a\right]\left[\tilde{N}\right] + \left[d\right]^{t}\left[\tilde{K}\right] \tag{1}$$

$$\left[\tilde{M}\right] = \left[d\right]\left[\tilde{N}\right] - \left[d^{*}\right]\left[\tilde{K}\right] \tag{2}$$

where $\left[\tilde{\epsilon}\right]$, $\left[\tilde{K}\right]$ represent strains and changes of curvature, while $\left[\tilde{N}\right]$ and $\left[\tilde{M}\right]$ are the resultant stresses and moments respectively. The definitions of elements in matrices $\left[a\right]$, $\left[d\right]$, and $\left[d^{*}\right]$ may be found in References 28 and 31.

2. EQUILIBRIUM AND COMPATIBILITY EQUATIONS

Corresponding to Donnell's strain-displacement relations, the equilibrium and compatibility equations for a composite cylindrical shell with reference surface radius R (see Figure 1) can be written as (Reference 28) two nonlinear differential equations,

$$\tilde{L}_1\left[\tilde{W}\right] - \tilde{L}_2\left[\tilde{F}\right] = \tilde{F}_{,\tilde{x}\tilde{x}}\,\tilde{W}_{,\tilde{y}\tilde{y}} + \tilde{F}_{,\tilde{y}\tilde{y}}\,\tilde{W}_{,\tilde{x}\tilde{x}} - 2\tilde{F}_{,\tilde{x}\tilde{y}}\,\tilde{W}_{,\tilde{x}\tilde{y}} \tag{3}$$

$$\tilde{L}_2\left[W\right] + \tilde{L}_3\left[\tilde{F}\right] = \left(\tilde{W}_{,\tilde{x}\tilde{y}}\right)^2 - \tilde{W}_{,\tilde{x}\tilde{x}}\,\tilde{W}_{,\tilde{y}\tilde{y}} \tag{4}$$

where $\tilde{W}$ is the radial displacement and $\tilde{F}$ is the Airy stress function. $\tilde{x}$ and $\tilde{y}$ represent the axial and the cirumferential coordinates on the reference surface respectively. The differential operators $\tilde{L}_i$ in Equations (3) and (4) are defined by

$$\tilde{L}_1\left[\ \right] = d_{11}^{*}\left[\ \right]_{,\tilde{x}\tilde{x}\tilde{x}\tilde{x}} + 4d_{16}^{*}\left[\ \right]_{,\tilde{x}\tilde{x}\tilde{x}\tilde{y}} + \left(2d_{12}^{*} + 4d_{66}^{*}\right)\left[\ \right]_{,\tilde{x}\tilde{x}\tilde{y}\tilde{y}}$$

$$+ 4d_{26}^{*}\left[\ \right]_{,\tilde{x}\tilde{y}\tilde{y}\tilde{y}} + d_{22}^{*}\left[\ \right]_{,\tilde{y}\tilde{y}\tilde{y}\tilde{y}}$$

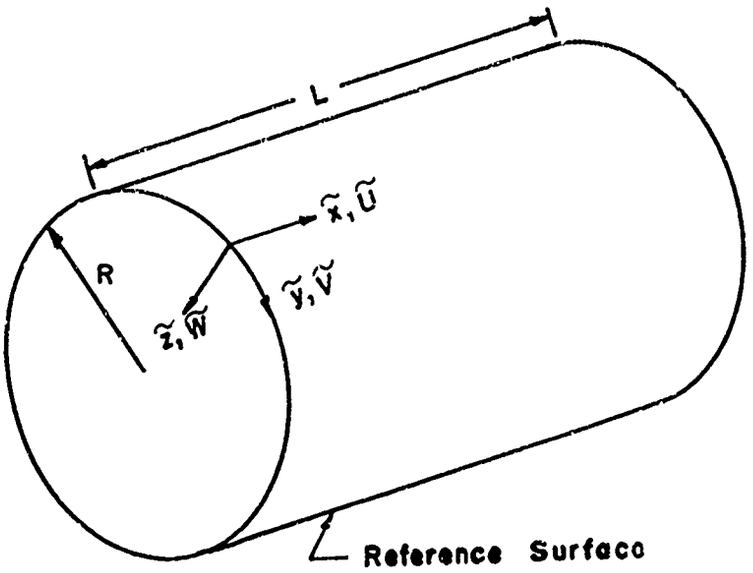

(a)

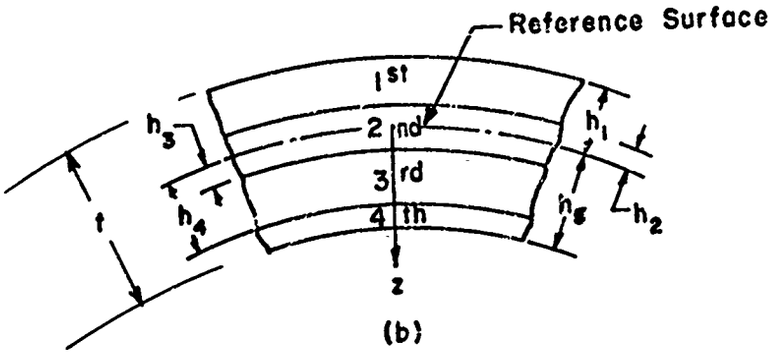

(b)

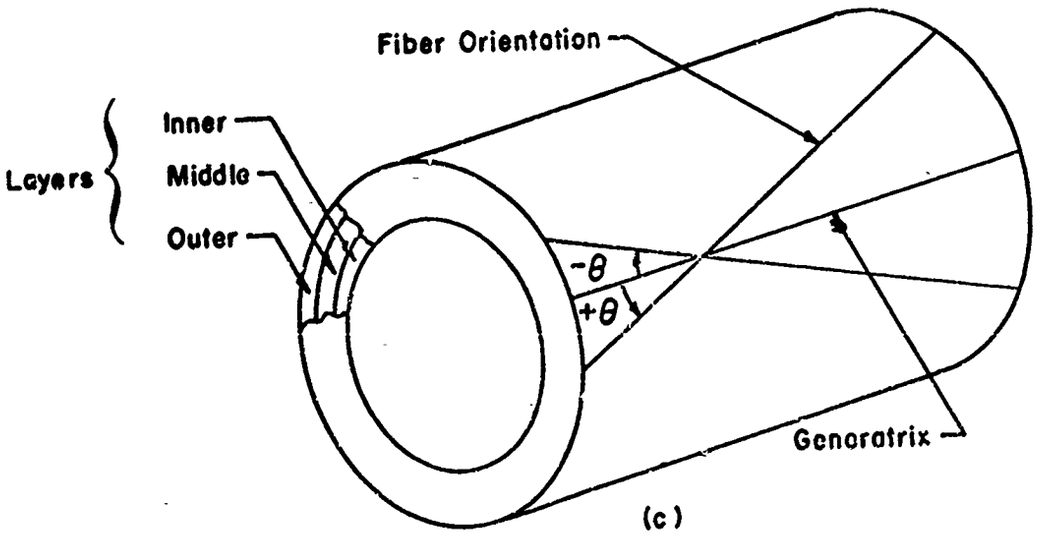

(c)

Figure 1. Geometry of the Shell

$$\tilde{L}_2[\,] = d_{12}[\,]_{,\tilde{x}\tilde{x}\tilde{x}\tilde{x}} + (2d_{62}-d_{16})[\,]_{,\tilde{x}\tilde{x}\tilde{x}\tilde{y}} + (d_{11}+d_{22}-2d_{66})[\,]_{,\tilde{x}\tilde{x}\tilde{y}\tilde{y}}$$
$$+(2d_{61}-d_{26})[\,]_{,\tilde{x}\tilde{y}\tilde{y}\tilde{y}} + d_{21}[\,]_{,\tilde{y}\tilde{y}\tilde{y}\tilde{y}} + \frac{1}{R}[\,]_{,\tilde{y}\tilde{y}} \qquad (5)$$

$$\tilde{L}_3[\,] = a_{22}[\,]_{,\tilde{x}\tilde{x}\tilde{x}\tilde{x}} - 2a_{26}[\,]_{,\tilde{x}\tilde{x}\tilde{x}\tilde{y}} + (2a_{12}+a_{66})[\,]_{,\tilde{x}\tilde{x}\tilde{y}\tilde{y}}$$
$$-2a_{16}[\,]_{,\tilde{x}\tilde{y}\tilde{y}\tilde{y}} + a_{11}[\,]_{,\tilde{y}\tilde{y}\tilde{y}\tilde{y}}$$

The coefficients a_{11}, d_{11}, d_{11}^*, d_{22}^*, etc. correspond to the elements of matrices $[a]$, $[d]$, and $[d^*]$ in Equations (1) and (2).

The nondimensional form of nonlinear Equations (3) and (4), which is used in the subsequent analysis, is given by

$$L_1[W] - L_2[F] = F_{,xx}W_{,yy} + F_{,yy}W_{,xx} - 2F_{,xy}W_{,xy} \qquad (6)$$

$$L_2[W] + L_3[F] = (W_{,xy})^2 - W_{,xx}W_{,yy} \qquad (7)$$

The linear differential operators in the above equations are defined as

$$L_1[\,] = \frac{\phi}{4}[\,]_{,xxxx} + \eta[\,]_{,xxxy} + \frac{\rho}{2}[\,]_{,xxyy}$$
$$+\zeta[\,]_{,xyyy} + \frac{\phi}{4}[\,]_{,yyyy}$$

$$L_2[\,] = \kappa[\,]_{,xxxx} + \nu[\,]_{,xxxy} + \psi[\,]_{,xxyy} + \xi[\,]_{,xyyy} \qquad (8)$$
$$+\bar{\lambda}[\,]_{,yyyy} + 2[\,]_{,xx}$$

$$L_3[\,] = \frac{4}{\phi}[\,]_{,xxxx} - \beta[\,]_{,xxxy} + 4\alpha[\,]_{,xxyy}$$
$$-\gamma[\,]_{,xyyy} + 4\phi[\,]_{,yyyy}$$

where

$$x = \tilde{x} / (4R^2 d_{11}^* a_{22})^{1/4} \qquad y = \tilde{y} / (4R^2 d_{22}^* a_{22})^{1/4}$$

$$N_x = \frac{\tilde{N}_x R}{2} \left(\frac{a_{11}}{d_{22}^*}\right)^{1/2} \qquad N_y = \frac{\tilde{N}_y R}{2} \frac{(a_{11} d_{11}^*)^{1/2}}{d_{22}^*}$$

$$N_{xy} = \frac{\tilde{N}_{xy} R}{2} \frac{a_{11}^{1/2} d_{11}^{*1/4}}{d_{22}^{*3/4}} \qquad \phi = \left(\frac{a_{11} d_{11}^*}{a_{22} d_{22}^*}\right)^{1/2}$$

$$\alpha = \frac{2a_{12} + a_{66}}{(a_{11} a_{22})^{1/2}} \qquad \beta = \frac{8a_{26}}{a_{11}^{1/4} a_{22}^{3/4}} \cdot \frac{1}{\sqrt{\phi}}$$

$$\gamma = \frac{8a_{16}}{a_{11}^{3/4} a_{22}^{1/4}} \sqrt{\phi} \qquad \xi = \frac{(2d_{61} - d_{26})}{(a_{22} d_{22}^*)^{1/2}} \left(\frac{a_{22}}{a_{11}}\right)^{1/4} \sqrt{\phi}$$

(9)

$$\kappa = \frac{d_{12}}{a_{22}} \left(\frac{a_{11}}{d_{22}^*}\right)^{1/2} \frac{1}{\phi} \qquad \bar{\lambda} = \frac{d_{21}}{(a_{11} d_{22}^*)^{1/2}} \phi$$

$$\nu = \frac{2d_{62} - 2d_{16}}{\sqrt{a_{22} d_{22}^*}} \sqrt[4]{\frac{a_{11}}{a_{22}}} \cdot \frac{1}{\phi^{1/2}} \qquad \eta = \frac{d_{16}^*}{d_{11}^{*3/4} d_{22}^{*1/4}} \phi$$

$$\zeta = \frac{d_{26}^*}{d_{11}^{*3/4} d_{22}^{*3/4}} \phi \qquad \psi = \frac{d_{11} + d_{22} - 2d_{66}}{(a_{22} d_{22}^*)^{1/2}}$$

$$\rho = \frac{d_{12}^* + 2d_{66}^*}{(d_{11}^* d_{22}^*)^{1/2}} \phi \qquad W = \tilde{W} / (a_{22} d_{22}^*)^{1/2} \qquad F = \tilde{F} \cdot \frac{1}{4} \cdot \frac{1}{d_{22}^*} \left(\frac{a_{11}}{a_{22}}\right)^{1/2}$$

The nondimensional stress resultants N_x, N_y, N_{xy} are related to the Airy stress function parameter F by

$$N_x = F_{,yy} \qquad N_y = F_{,xx} \qquad N_{xy} = -F_{,xy} \tag{10}$$

3. INITIAL POSTBUCKLING BEHAVIOR

A short discussion and the essential equations pertaining to initial postbuckling behavior of a structure are given here. A detailed derivation of these equations and the discussion on the basic assumptions involved may be found in References 1 through 5. It has been shown by Koiter that the imperfection sensitivity of a structure depends on the initial postbuckling behavior of a perfect structure. This behavior is represented by the relation

$$\frac{\lambda}{\lambda_c} = 1 + a\epsilon + b\epsilon^2 \tag{11}$$

where λ_c is the particular value of the load parameter λ at the classical buckling load. A perfect structure may be defined as the one which possesses a bifurcation point whereas the imperfect structure buckles in snap-through buckling mode. In Equation (11) ϵ is a perturbation coefficient which can be considered to represent the contribution by the classical buckling mode to the buckled state (see Equation 17). The behavior of a structure represented by Equation (11) is shown in Figures 2a, 2b, and 2c. The initial postbuckling behavior is independent of the sign of the buckling mode when a = 0. Then, this behavior depends only on the parameter "b" and its value determines the nature of the imperfection sensitivity. For instance when $b > 0$ and $a = 0$ the structure is not sensitive to initial imperfection and λ increases after buckling (Figure 2b). In case b is zero and $a = 0$ the parameter λ remains the same as λ_c in the initial postbuckling region. In case $b < 0$ and $a = 0$, λ decreases after buckling (Figure 2c). When $a \neq 0$ λ increases or decreases depending upon the sign of the buckling mode.

If the initial geometric deviations are assumed to have the same form as the classical buckling mode, the equilibrium equation in the initial postbuckling region assumes the following form

$$\left(1 - \frac{\lambda}{\lambda_c}\right)\epsilon + b\epsilon^2 = \frac{\lambda}{\lambda_c}\,\overline{W}^* \tag{12}$$

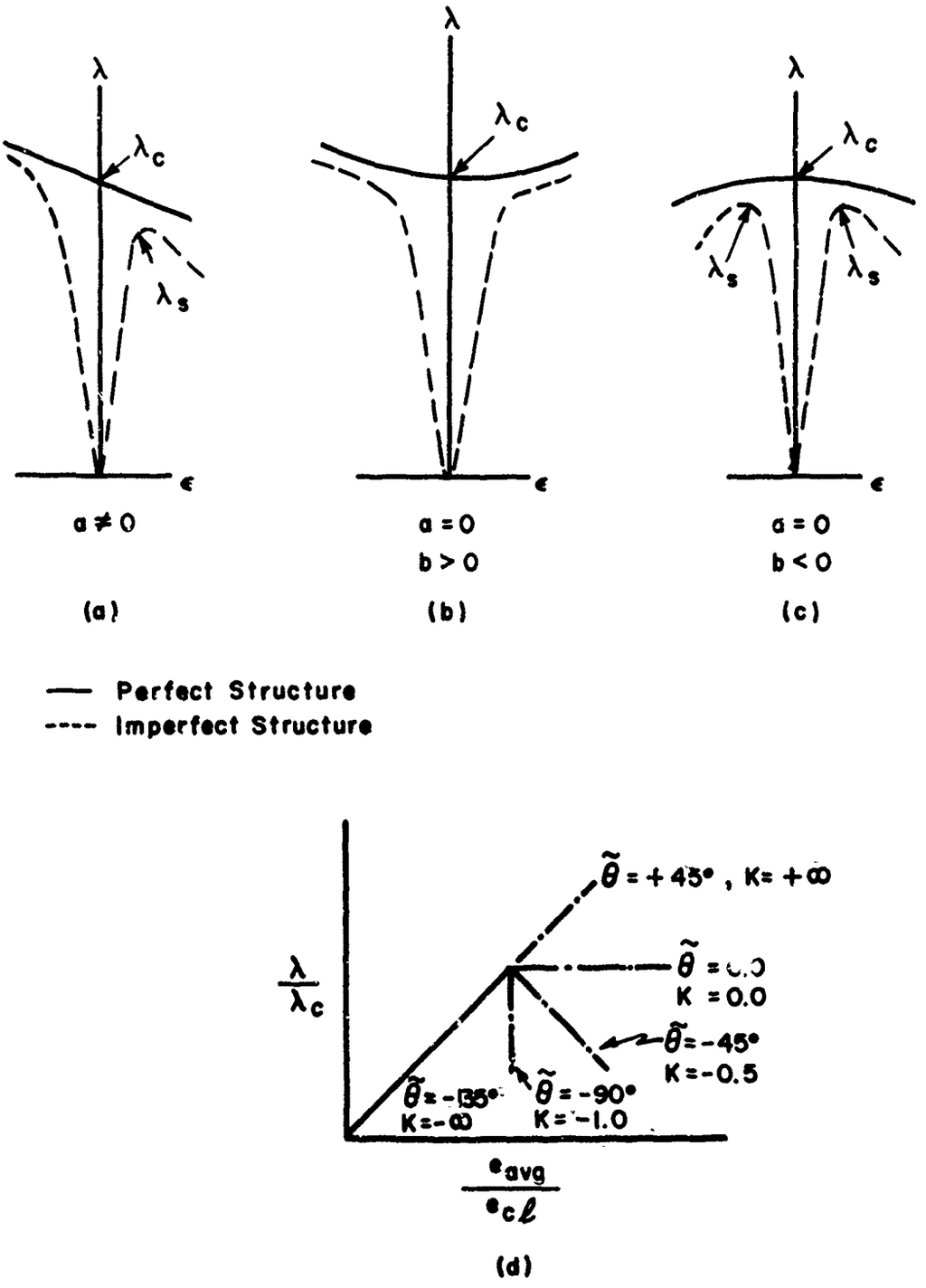

Figure 2. Load-Deflection Curves

where $\overline{W}^*$ is the ratio of the amplitudes of the initial imperfection ($\overline{h}$) to the radial displacement (h). An expression relating the buckling load parameters of the imperfect structure (λ_s) and the perfect structure (λ_c) can be obtained from Equation (12) by utilizing the condition, $\left.\frac{d\lambda}{d\epsilon}\right|_{\lambda=\lambda_s} = 0$. The relation is

$$\left(1-\frac{\lambda_s}{\lambda_c}\right)^{3/2} = \frac{3\sqrt{3}}{2}\sqrt{-b}\,\left|\overline{W}^*\right|\,\frac{\lambda_s}{\lambda_c} \tag{13}$$

The relation between end-shortening and the applied load in the initial post-buckling region for a perfect structure is given by

$$\frac{e_{avg}}{e_{c\ell}} = \frac{\lambda}{\lambda_c} + \frac{1}{K}\left(\frac{\lambda}{\lambda_c}-1\right) \tag{14}$$

where e_{avg} is the average end-shortening and $e_{c\ell}$ is the prebuckling axial end-shortening at the classical buckling load (see Figure 2d). The angle of the initial slope ($\tilde{\theta}$) of the load vs end-shortening curve is related to the coefficient K in Equation (14) by

$$\theta = \tan^{-1}\left(\frac{K}{K+1}\right) \tag{15}$$

The information regarding the initial slope of the load vs end-shortening curve is helpful in determining whether the buckling will be gradual or catastrophic.

4. INITIAL POSTBUCKLING ANALYSIS OF A PERFECT CYLINDRICAL SHELL

The analysis presented in this section is based on Koiter's general theory (References 1 through 6).

If the prebuckling displacements are neglected then the prebuckling stresses are linearly related to the load parameter λ. Then

$$\lambda \overset{\bullet}{N}_x = \lambda \overset{\bullet}{F}_{,yy} = -\lambda\left[\overset{\circ}{\tilde{N}}_x\right]\frac{R}{2}\left(\frac{a_{11}}{d^*_{22}}\right)^{1/2}$$

$$\lambda \overset{\bullet}{N}_y = \lambda \overset{\bullet}{F}_{,xx} = \lambda\left[-\tilde{p}\,R\right]\frac{R}{2}\,\frac{(a_{11}\,d^*_{11})^{1/2}}{d^*_{22}} \tag{16}$$

$$\lambda \overset{\circ}{N}_{xy} = -\lambda \overset{\circ}{F}_{,xy} = \lambda \left[\tilde{\tau}\right] \frac{R}{2} \frac{a_{11}^{1/2} \, d_{11}^{*1/4}}{d_{22}^{*3/4}}$$

where $\overset{\circ}{\tilde{N}}_x$ is the axially applied compressive load per unit length of the circumference, $\tilde{p}$ is the external radial pressure, and $\tilde{\tau}$ is the applied torsion.

In the following analysis it is assumed that the classical buckling load parameter λ_c is associated with a unique buckling mode $\overset{(1)}{W}$ and the corresponding stress function $\overset{(1)}{F}$. In order to investigate how the structure behaves immediately after the buckling the functions W and F are expanded in the following form,

$$W = \epsilon \overset{(1)}{W} + \epsilon^2 \overset{(2)}{W} + \epsilon^3 \overset{(3)}{W} + \cdots\cdots$$

$$F = \lambda \overset{\circ}{F} + \epsilon \overset{(1)}{F} + \epsilon^2 \overset{(2)}{F} + \cdots\cdots \qquad (17)$$

Substitution of the above relations in the nonlinear Equations (6) and (7) generates a set of linear differential equations. Keeping in mind that $\lambda \to \lambda_c$ as $\epsilon \to 0$, we note the first set of equations corresponding to the classical buckling mode $\overset{(1)}{W}$ and the stress function $\overset{(1)}{F}$ are

$$L_1\left[\overset{(1)}{W}\right] - L_2\left[\overset{(1)}{F}\right] = \lambda_c\left[\overset{\circ}{F}_{,xx} \overset{(1)}{W}_{,yy} + \overset{\circ}{F}_{,yy} \overset{(1)}{W}_{,xx} - 2\overset{\circ}{F}_{,xy} \overset{(1)}{W}_{,xy}\right] \qquad (18)$$

$$L_2\left[\overset{(1)}{W}\right] + L_3\left[\overset{(1)}{F}\right] = 0.0 \qquad (19)$$

After obtaining the solution to the above set, it is necessary to solve the second set of equations corresponding to $\overset{(2)}{W}$ and $\overset{(2)}{F}$. The equations are

$$L_1\left[\overset{(2)}{W}\right] - L_2\left[\overset{(2)}{F}\right] - \lambda_c\left[\overset{\circ}{F}_{,xx} \overset{(2)}{W}_{,yy} + \overset{\circ}{F}_{,yy} \overset{(2)}{W}_{,xx} - 2\overset{\circ}{F}_{,xy} \overset{(2)}{W}_{,xy}\right]$$
$$= \overset{(1)}{F}_{,xx} \overset{(1)}{W}_{,yy} + \overset{(1)}{F}_{,yy} \overset{(1)}{W}_{,xx} - 2\overset{(1)}{F}_{,xy} \overset{(1)}{W}_{,xy} \qquad (20)$$

$$L_2\left[\overset{(2)}{W}\right] + L_3\left[\overset{(2)}{F}\right] = \left(\overset{(1)}{W}_{,xy}\right)^2 - \overset{(1)}{W}_{,xx} \overset{(1)}{W}_{,yy} \qquad (21)$$

The general expressions for the initial postbuckling coefficients "a" and "b" in Equation (11) can be evaluated once the functions $\overset{(1)}{W}$, $\overset{(1)}{F}$ and $\overset{(2)}{W}$, $\overset{(*)}{F}$ are known. They are given by (Reference 6)

$$a = \frac{\frac{3}{2}\iint \left[\overset{(1)}{F}_{,xx}(\overset{(1)}{W}_{,y})^2 + \overset{(1)}{F}_{,yy}(\overset{(1)}{W}_{,x})^2 - 2\overset{(1)}{F}_{,xy}\overset{(1)}{W}_{,x}\overset{(1)}{W}_{,y}\right] dxdy}{-\lambda_c \iint \left[\overset{\circ}{F}_{,xx}\overset{(1)}{W}_{,y} + \overset{\circ}{F}_{,yy}\overset{(1)}{W}_{,x} - 2\overset{\circ}{F}_{,xy}\overset{(1)}{W}_{,x}\overset{(1)}{W}_{,y}\right] dxdy} \tag{22}$$

$$b = \frac{\begin{array}{l} 2\iint \left[\overset{(1)}{F}_{,xx}\overset{(1)}{W}_{,y}\overset{(2)}{W}_{,y} + \overset{(1)}{F}_{,yy}\overset{(1)}{W}_{,x}\overset{(2)}{W}_{,x} - \overset{(1)}{F}_{,xy}\left\{\overset{(1)}{W}_{,x}\overset{(2)}{W}_{,y} + \overset{(1)}{W}_{,y}\overset{(2)}{W}_{,x}\right\}\right] dxdy \\ +\iint \left[\overset{(2)}{F}_{,xx}(\overset{(1)}{W}_{,y})^2 + \overset{(2)}{F}_{,yy}(\overset{(1)}{W}_{,x})^2 - 2\overset{(2)}{F}_{,xy}\overset{(1)}{W}_{,x}\overset{(1)}{W}_{,y}\right] dxdy \end{array}}{-\lambda_c \iint \left[\overset{\circ}{F}_{,xx}(\overset{(1)}{W}_{,y})^2 + \overset{\circ}{F}_{,yy}(\overset{(1)}{W}_{,x})^2 - 2\overset{\circ}{F}_{,xy}\overset{(1)}{W}_{,x}\overset{(1)}{W}_{,y}\right] dxdy} \tag{23}$$

When the coefficients "a" and "b" are known, Equations (11) through (15) can be used to study the initial postbuckling behavior.

5. CLASSICAL BUCKLING LOAD

The radial displacement parameter corresponding to the classical buckling mode for the perfect cylindrical shell is presented by

$$\overset{(1)}{W} = h \sin \frac{m\pi x}{\ell} \cos \frac{n}{r}(y - \tau x) \tag{24}$$

where 2m and n are the number of waves in the longitudinal and circumferential directions respectively. The parameter τ is introduced to take into account the coupling between the changes of curvature $\tilde{k}_x$, $\tilde{k}_y$ and the torsion $\tilde{k}_{xy}$ in the bending stiffness matrix $[d^*]$ (see Equation 2). Equation (24) due to the introduction of τ may also be used when the shell is subjected to torsional load. In this analysis the boundary conditions at the ends of the shell are not applied. In Equation (24) the parameters h, r, and ℓ are related to the thickness of the shell t, the radius R, and the length L by

$$h = \frac{t}{(a_{22}d^*_{22})^{1/2}} \qquad r = \frac{R}{(4R^2 d^*_{22} a_{22})^{1/4}} \qquad \ell = \frac{L}{(4R^2 d^*_{11} a_{22})^{1/4}} \tag{25}$$

Equation (24) can also be written in the following different form

$$\overset{(1)}{W} = \frac{h}{2} \left\{ \sin (M_x - N_y) + \sin (P_x + N_y) \right. \tag{26}$$

where

$$M = \frac{m\pi}{\ell} + \frac{n}{r}\tau \qquad N = \frac{n}{r} \qquad P = \frac{m\pi}{\ell} - \frac{n}{r}\tau \tag{27}$$

The compatibility relation defined by Equation (19) can be solved exactly for the stress function $\overset{(1)}{F}$ in terms of the assumed buckling mode $\overset{(1)}{W}$. This gives

$$\overset{(1)}{F} = -\frac{h}{2}\frac{T_3}{T_5} \sin (M_x - N_y) - \frac{h}{2}\frac{T_4}{T_6} \sin (P_x + N_y) \tag{28}$$

where

$$\begin{aligned} T_3 &= \kappa M^4 - \nu M^3 N + \psi M^2 N^2 - \xi N^3 M + \bar{\lambda} N^4 - 2M^2 \\ T_5 &= \frac{4}{\phi} M^4 + \beta M^3 N + 4\alpha M^2 N^2 + \gamma M N^3 + 4\phi N^4 \end{aligned} \tag{29}$$

T_4 and T_6 are obtained from T_3 and T_5 respectively by replacing M by - P.

The classical buckling load parameter λ_c is the lowest of all the eigenvalues resulting from the expression obtained by substituting the functions $\overset{(1)}{W}$ and $\overset{(1)}{F}$ in Equation (18). This gives

$$\begin{aligned} \lambda_c \left[\dot{N}_x (M^2 + P^2) + 2\dot{N}_y N^2 + 2\dot{N}_{xy} (P - M) N \right] \\ = -\left[T_1 + T_2 + \frac{T_3^2}{T_5} + \frac{T_4^2}{T_6} \right] \end{aligned} \tag{30}$$

where

$$T_1 = \frac{\phi}{4} M^4 - \eta M^3 N + \frac{\rho}{2} M^2 N^2 - \xi M N^3 + \frac{\phi}{4} N^4$$

and T_2 is obtained from T_1 by replacing M by - P.

When the cylindrical shell is subjected to axial load alone, Equation (30) reduces to

$$\lambda_c \dot{N}_x = -\frac{1}{M^2 + P^2} \left[T_1 + T_2 + \frac{T_3^2}{T_5} + \frac{T_4^2}{T_6} \right] \tag{31}$$

The numerical results presented in this report are for a shell subjected to axial load only. In order to evaluate the buckling load one can assume $\lambda_c = 1$ and

minimize $\overset{o}{N}_x$ with respect to M, P, and τ. In evaluating the classical buckling loads m and n are assumed to be integers and τ noninteger. When $\tau = 0$, it can be shown that Equation (31) is the same as the corresponding expression in Reference 28, which was obtained from the principle of minimum potential energy.

6. EVALUATION OF COEFFICIENTS "a" AND "b"

Since the coefficient "a" in Equation (22) depends on $\overset{(1)}{W}$ and $\overset{(1)}{F}$ alone, it can be shown that it is equal to zero for the present case. In order to calculate "b" according to Equation (23) it is necessary to solve Equations (20) and (21).

The right side of Equations (20) and (21) which involve the functions $\overset{(1)}{W}$ and $\overset{(1)}{F}$ are given by

$$-\frac{h^2}{4}\left[\frac{T_5}{T_5}+\frac{T_6}{T_6}\right]N^2\,(M+P)^2\sin(M_x-N_y)\sin(P_x+N_y) \tag{32}$$

and

$$-\frac{h^2}{4}\left[M+P\right]^2 N^2\sin(M_x-N_y)\sin(P_x+N_y) \tag{33}$$

respectively. The solution to the simultaneous set of Equations (20) and (21) is assumed to have the following form

$$\overset{(2)}{W} = \sum_{i=1,3,5,\cdots}\alpha_i \sin\frac{i\pi x}{\ell} + \frac{1}{2}\cos\frac{2ny}{r}\sum_{i=1,3,5,\cdots}\gamma_i\left\{\sin M_i x + \sin P_i x\right\}$$

$$+\frac{1}{2}\sin\frac{2ny}{r}\sum_{i=1,3,5,\cdots}\gamma_i\left\{\cos P_i x - \cos M_i x\right\} \tag{34}$$

$$\overset{(2)}{F} = \sum_{i=1,3,5,\cdots}\beta_i \sin\frac{i\pi x}{\ell} + \frac{1}{2}\cos\frac{2ny}{r}\sum_{i=1,3,5,\cdots}\delta_i\left\{\sin M_i x + \sin P_i x\right\}$$

$$+\frac{1}{2}\sin\frac{2ny}{r}\sum_{i=1,3,5,\cdots}\delta_i\left\{\cos P_i x - \cos M_i x\right\} \tag{35}$$

where $\alpha_i, \beta_i, \gamma_i, \delta_i$ are the unknown coefficients and

$$M_i = \frac{i\pi}{\ell} + \frac{2n\tau}{r} \qquad P_i = \frac{i\pi}{\ell} - \frac{2n\tau}{r}$$

The coefficients of the series in Equations (34) and (35) can be obtained by Galerkin's method. This gives

$$\alpha_i = \frac{\frac{2h^2N^2m^2}{(i^2-4m^2)}\ \frac{\pi i}{\ell^2}\left\{\left(\frac{T_3}{T_5}+\frac{T_4}{T_6}\right)\ \frac{4}{\phi} + \kappa - 2\left(\frac{\ell}{i\pi}\right)^2\right\}}{\left(\frac{i\pi}{\ell}\right)^4 + \lambda_c \mathring{N}_x \frac{4}{\phi}\left(\frac{i\pi}{\ell}\right)^2 + \left\{\kappa\left(\frac{i\pi}{\ell}\right)^2 - 2\right\}^2} \tag{36}$$

$$\beta_i = \phi\left[\frac{h^2N^2m^2}{(i^2-4m^2)}\ \frac{\pi i}{2\ell^2}\ \left(\frac{\ell}{i\pi}\right)^4 - \alpha_i\left\{\frac{\kappa}{4} - \frac{1}{2}\left(\frac{\ell}{i\pi}\right)^2\right\}\right] \tag{37}$$

$$\gamma_i = \frac{\frac{-4h^2N^2m^2\pi^2}{\ell^2}\cdot\frac{1}{i\pi}\left\{\left(\frac{T_3}{T_5}+\frac{T_4}{T_6}\right)\ T_9 + T_8\right\}}{T_7\cdot T_9 + T_8^2} \tag{38}$$

$$\delta_i = -\left[\frac{4h^2N^2m^2\pi^2}{\ell^2}\cdot\frac{1}{i\pi} + \gamma_i\ T_8\right]\frac{1}{T_9} \tag{39}$$

where

$$T_7 = \frac{\phi}{4}\ (M_i^4 + P_i^4) - \eta\left(\frac{2n}{r}\right)(M_i^3 - P_i^3) + \frac{\rho}{2}\left(\frac{2n}{r}\right)^2(M_i^2+P_i^2)$$

$$-\zeta\left(\frac{2n}{r}\right)^3(M_i - P_i) + \frac{\phi}{2}\left(\frac{2n}{r}\right)^4 + \lambda_c\left[\mathring{N}_x\left\{M_i^2 + P_i^2\right\}\right.$$

$$\left. + 2\mathring{N}_y\left(\frac{2n}{r}\right)^2 - 2\mathring{N}_{xy}\left\{M_i - P_i\right\}\frac{2n}{r}\ \right]$$

$$T_8 = \kappa\ (M_i^4 + P_i^4) - \nu\left(\frac{2n}{r}\right)\ (M_i^3 - P_i^3) + \psi\left(\frac{2n}{r}\right)\ (M_i^2 + P_i^2)$$

$$-\xi\left(\frac{2n}{r}\right)^3\ (M_i + P_i) + 2\bar{\lambda}\left(\frac{2n}{r}\right)^4 - 2\ (M_i^2 + P_i^2)$$

$$T_9 = \frac{4}{\phi}\left(M_i^4 + P_i^4\right) - \beta\left(\frac{2n}{r}\right)\left(M_i^3 - P_i^3\right) + 4\alpha\left(\frac{2n}{r}\right)^2\left(M_i^2 + P_i^2\right)$$

$$- \gamma\left(\frac{2n}{r}\right)^3\left(M_i - P_i\right) + 8\phi\left(\frac{2n}{r}\right)^4$$

The condition that the circumferential displacement $\tilde{V}$ be single valued is equivalent to $\int_0^{2\pi R} \tilde{V}_{,\tilde{y}}\, d\tilde{y} = 0$. For $\overset{(2)}{\tilde{V}}$ a term in the expansion of $\tilde{V}$ similar to Equation 17, this condition is equivalent to

$$\int_0^{2\pi R} \Big[a_{12}\overset{(2)}{\tilde{F}}_{,yy} + a_{22}\overset{(2)}{\tilde{F}}_{,xx} - a_{26}\overset{(2)}{\tilde{F}}_{,xy} + d_{12}\overset{(2)}{\tilde{W}}_{,xx} + d_{22}\overset{(2)}{\tilde{W}}_{,yy} + 2d_{62}\overset{(2)}{\tilde{W}}_{,xy} - \frac{1}{2}\left(\overset{(1)}{\tilde{W}}_{,y}\right)^2 + \frac{\overset{(2)}{\tilde{W}}}{R} \Big]\, d\tilde{y} = 0 \qquad (40)$$

It can be shown that this condition is satisfied in the present case.

Substituting $\overset{(1)}{W}$, $\overset{(1)}{F}$, $\overset{(2)}{W}$, and $\overset{(2)}{F}$ in Equation (23) results in the following expression

$$b = \frac{4N^2 m^2 \pi}{\lambda_c \ell^2} \cdot \frac{S_1}{S_2} \qquad (41)$$

where

$$S_1 = \left\{\frac{T_3}{T_5} + \frac{T_4}{T_6}\right\}\left\{\sum_{i=1,3,5,\cdots} \alpha_i \frac{2i}{i^2 - 4m^2} - \sum \frac{\gamma_i}{i}\right\}$$

$$- \sum_{i=1,3,5,\cdots} \beta_i \frac{2i}{i^2 - 4m^2} + \sum_{i=1,3,5,\cdots} \frac{\delta_i}{i} \qquad (42)$$

and

$$S_2 = \mathring{N}_x\left\{\left(\frac{m\pi}{\ell}\right)^2 + N^2\tau^2\right\} + \mathring{N}_y N^2 - 2\mathring{N}_{xy} N^2 \tau \qquad (43)$$

7. INITIAL SLOPE OF LOAD VS END-SHORTENING CURVE

The average end-shortening is given by

$$e_{avg} = \frac{1}{2\pi R}\int_0^L \int_0^{2\pi R} \tilde{U}_{,x}\, d\tilde{x}\, d\tilde{y} \qquad (44)$$

$$= \frac{1}{2\pi R}\int_0^L \int_0^{2\pi R} \left(\tilde{\epsilon}_x - \frac{1}{2}\left(\tilde{W}_{,\tilde{x}}\right)^2\right) d\tilde{x}\, d\tilde{y} \qquad (45)$$

where $\tilde{u}$ is the axial displacement. The relation between the end-shortening and the load can be obtained from the expansion

$$e = \lambda \overset{\circ}{e} + \epsilon \overset{(1)}{e} + \epsilon^2 \overset{(2)}{e} \tag{46}$$

Since

$$\lambda \rightarrow \lambda_c \quad \text{and} \quad e \rightarrow e_{c\ell} \quad \text{as} \quad \epsilon \rightarrow 0$$

$$e_{c\ell} = \lambda_c \overset{\circ}{e} \tag{47}$$

where $e_{c\ell}$ is the prebuckling end-shortening at the classical buckling load. For a = 0 corresponding to the present case Equation (9) gives

$$\epsilon^2 \approx -\left(1 - \frac{\lambda}{\lambda_c}\right) b \tag{48}$$

By use of Equation (1) and (45) through (48), the following relation is obtained

$$\frac{e_{avg}}{e_{c\ell}} = \frac{\lambda}{\lambda_c} + \frac{1}{K}\left(\frac{1}{\lambda_c} - 1\right) \tag{49}$$

where

$$\frac{1}{K} = \frac{1}{b} \frac{\int_0^L \int_0^{2\pi R} \left\{ a_{12} \overset{(2)}{\tilde{F}}_{,\tilde{x}\tilde{x}} + d_{11} \overset{(2)}{\tilde{W}}_{,\tilde{x}\tilde{x}} - \frac{1}{2} \left(\overset{(1)}{\tilde{W}}_{,x} \right)^2 \right\} d\tilde{x}\, d\tilde{y}}{\int_0^L \int_0^{2\pi R} \left[a_{11} \overset{\circ}{\tilde{F}}_{,yy} + a_{12} \overset{\circ}{\tilde{F}}_{,xx} - a_{13} \overset{\circ}{\tilde{F}}_{,xy} \right] d\tilde{x}\, d\tilde{y}} \tag{50}$$

Utilizing Equation (9) one gets

$$\frac{1}{K} = \frac{\frac{1}{b} \int_0^{\ell} \int_0^{2\pi r} \left[\frac{a_{12} d_{22}^*}{\sqrt{a_{11} d_{11}^*}} \overset{(2)}{F}_{,xx} + \frac{d_{11}}{4} \left(\frac{d_{22}^*}{d_{11}^*} \right)^{1/2} \overset{(2)}{W}_{,xx} - \frac{1}{8} d_{22}^* \left(\frac{a_{22}}{d_{11}^*} \right)^{1/2} \overset{(1)}{W}_{,x}{}^2 \right] dx\, dy}{\int_0^{\ell} \int_0^{2\pi r} \left[a_{11} \left(\frac{d_{22}^*}{a_{11}} \right)^{1/2} \overset{\circ}{N}_x + a_{12} \frac{d_{22}^*}{\sqrt{a_{11} d_{11}^*}} \overset{\circ}{N}_y + a_{13} \frac{d_{22}^{*3/4}}{a_{11}^{*1/2} d_{11}^{*3/4}} \overset{\circ}{N}_{xy} \right] dx\, dy} \tag{51}$$

From Equation (49) it can be shown that in the initial postbuckling region the slope of the load vs end-shortening curve is given by

$$\tan \tilde{\theta} = \frac{K}{K+1} \tag{52}$$

Using Equations (24), (34), and (35), Equation (51) can be written as

$$\frac{1}{b}\left[-\frac{a_{12}d_{22}^*}{\sqrt{a_{11}\,d_{11}^*}}\,\frac{4\pi^2 r}{\ell}\sum_{i=1,3,5,\cdots}\beta_i\,i-\frac{d_{11}}{4}\sqrt{\frac{d_{22}^*}{d_{11}^*}}\,\frac{4\pi^2 r}{\ell}\sum_{i=1,3,5,\cdots}\alpha_i\,i\right.$$

$$\left.-\frac{1}{8}\,d_{22}^*\sqrt{\frac{a_{22}}{d_{11}^*}}\,\frac{h^2\pi r\ell}{2}\left(\frac{m^2\pi^2}{\ell^2}+N^2\tau^2\right)\right]$$

$$\frac{1}{K}=\frac{}{2\pi r\ell\left[a_{11}\sqrt{\frac{d_{22}^*}{a_{11}}}\,\mathring{N}_x+a_{12}\,\frac{d_{22}^*}{\sqrt{a_{11}\,d_{11}^*}}\,\mathring{N}_y+a_{13}\,\frac{d_{22}^{*\,3/4}}{a_{11}^{1/2}\,d_{11}^{*\,1/4}}\,\mathring{N}_{xy}\right]} \tag{53}$$

8. INFLUENCE OF INITIAL GEOMETRIC DEVIATION ON BUCKLING LOAD

In the present analysis the initial geometric deviation of the cylindrical shell is taken to be

$$\bar{W}=\bar{h}\,\sin\frac{m\pi x}{\ell}\,\cos\frac{n}{r}\,(y-\tau x) \tag{54}$$

where $\bar{h}$ is the amplitude of initial imperfection. As mentioned in Section III, when the initial geometric deviation has the same form as the classical buckling mode, the relation between the classical buckling load parameter λ_c and the buckling parameter load of an imperfect structure λ_s is given by

$$\left(1-\frac{\lambda_s}{\lambda_c}\right)^{3/2}=\frac{3\sqrt{3}}{2}\sqrt{-b}\,\left|\bar{W}^*\right|\frac{\lambda_s}{\lambda_c} \tag{55}$$

(also Eq 13)

where $\bar{W}^*$ is the ratio of the amplitude of initial deviation to the thickness of the shell, i.e., $\bar{W}^*=\frac{\bar{h}}{h}$. For a given shell once the coefficient "b" is obtained, Equation (55) can be used to evaluate the buckling load of an imperfect shell λ_s for a specified value of $\bar{W}^*$. Since Equation (55) is nonlinear, a method similar to Newton-Raphson technique can be used to evaluate λ_s/λ_c for a given $\bar{W}^*$.

9. CALCULATIONS

For computations, a Fortran IV program was written for the IBM 7094 digital computer. Since "b" and "K" are defined as the sum of a series, the summation was continued until the difference between the consecutive values

is less than 10^{-5}. The output from this portion of the program was used to evaluate λ_s and the corresponding buckling load parameter $\bar{N}_x$ for different values of the imperfection parameter $\bar{W}^*$. From Equation (6), it is seen that the buckling load $\overset{o}{\bar{N}}_x$ is related to buckling load parameter $\bar{N}_x$ as follows

$$\bar{N}_x = \frac{\overset{o}{\bar{N}}_x R}{2} \left(\frac{a_{11}}{d_{22}^*}\right)^{1/2} \tag{56}$$

SECTION III

NUMERICAL RESULTS AND CONCLUSIONS

1. NUMERICAL RESULTS

The behavior of a composite cylindrical shell is a function of a) elastic constants of the material, b) geometry of the shell (radius, thickness, and length), c) number of layers, and d) fiber orientation in each layer. A three-layer cylindrical shell of radius 6.0 inches and thickness of 0.036 inch is considered. The thickness of each layer is 0.012 inch. The shell is of either glass-epoxy or boron-epoxy composites. The elastic constants of the composites are as given below.

glass-epoxy	boron-epoxy
$E_{11} = 7.5 \times 10^6$ psi	$E_{11} = 40.0 \times 10^6$ psi
$E_{22} = 3.5 \times 10^6$ psi	$E_{22} = 4.5 \times 10^6$ psi
$\nu_{12} = 0.25$	$\nu_{12} = 0.25$
$G = 1.25 \times 10^6$ psi	$G = 1.5 \times 10^6$ psi

$$\nu_{21} = \nu_{12} E_{22}/E_{11}$$

Two sets of fiber orientations are chosen to illustrate the effect of fiber orientation on the buckling load and on the initial postbuckling behavior. The fiber orientations in outer, middle, and inner layers are 1) $\theta^\circ, -\theta^\circ, 0^\circ$ and 2) $\theta^\circ, -\theta^\circ, 90^\circ$ respectively for the two sets. The value of θ is varied from 0° to 90° at ten degree increments. The results of the twenty cylinders are compared. For convenience the two sets will be referred to as 1. θ and 2. θ and the value of θ will indicate the corresponding fiber orientation. For illustration, 2.30 will correspond to the fiber orientation (30°, -30°, 90°). The convention used in defining the angle θ is shown in Figure 1. When θ is 0° all fibers are axially oriented and when θ is 90° all fibers are circumferentially oriented.

The results are presented in Figures 1 through 14 and also tabulated in Appendixes I and II. The variation of coefficients "b" and "K" and the angle $\tilde{\theta}$ for the two sets of fiber orientations are plotted in Figures 3 through 5. The curves for glass-epoxy and boron-epoxy are shown on the same figure to

illustrate the effect of elastic properties of the material. As mentioned before the behavior of the structure is determined by the coefficients "b" and "K" or the angle $\tilde{\theta}$. The coefficient "b" indicates the degree of imperfection sensitivity and the angle $\tilde{\theta}$ shows how the failure would occur. From Figure 3 it can be seen that the magnitude of "b" is found to be greater for glass-epoxy than that for boron-epoxy (see Figure 3). This indicates that the glass-epoxy shells are more imperfection sensitive than the boron-epoxy shells. A similar conclusion was reached in Reference 29, where the results were obtained from a different analytical approach. For both materials as the fiber orientation angle θ changes from 0° to 90°, the coefficient "b" increases until θ reaches 40° and then it decreases.

The topmost curves in Figures 6 and 8 show the variation of classical buckling load with the fiber orientations in sets 1 and 2 respectively for glass-epoxy shells. Similarly the topmost curves of Figures 10 and 12 give classical buckling loads for boron-epoxy shells. For these curves the imperfection parameter $\overline{W}^*$ is zero. A comparison of the variation of "b" and the classical buckling load with the fiber orientations reveals that an increase in classical buckling load is accompanied by an increase in imperfection sensitivity. This shows that a shell with an efficient arrangement of fiber orientation with greater classical buckling load will be highly imperfection sensitive. In practice, it may be advisable to balance these two aspects in order to obtain an optimum design.

Figure 4 shows the variation of the coefficient "K" for the two sets of fiber orientations. The initial slope $\tilde{\theta}$ of the load vs end-shortening curve is plotted in Figure 5 as a function of fiber orientation for the two materials. This figure indicates that the angle $\tilde{\theta}$ for glass-epoxy is not significantly affected by the fiber orientation, but the high negative value suggests that the buckling of a nearly perfect shell under prescribed end-shortening will not be gradual but sudden. However, for boron-epoxy the angle varies with the change in fiber orientation, and whether the failure is catastrophic or not depends on the fiber orientation.

The effect of initial geometric deviation on the buckling load is illustrated in Figures 6 through 13. In Figures 6, 8, 10, and 11 the variation of buckling load $\overline{N}_x^o$ with change in fiber orientation and the imperfection parameter $\overline{W}^*$ is indicated, while in Figures 7, 9, 12, and 13 the variation of the ratio $\rho^* = \lambda_s/\lambda_c$

is considered. As mentioned before the topmost curves in Figures 6, 8, 10, and 11 correspond to the classical buckling load, where the imperfection parameter $\overline{W}^* = 0$. The curve for classical buckling load is characterized by a bump at intermediate values of θ. For smaller value of $\overline{W}^*$, the shape of the curve is similar to the curve corresponding to the classical buckling load. However, the curve is flattened for large values of $\overline{W}^*$. It is interesting to note that when $\overline{W}^* = 1.0$ the buckling load corresponding to intermediate values of θ is smaller than that at θ equal to zero (see Figure 12).

In Figure 14, the results obtained by the theory developed in this report are compared with those in Reference 32. In Reference 32 the buckling load of an imperfect shell was obtained from the principle of stationary potential energy. The radial displacement as well as the initial imperfection was represented by a four term expression. From Figure 14 it is seen that both theories give nearly the same results for small values of $\overline{W}^*$. For large values of $\overline{W}^*$ the method used in Reference 32 was not able to evaluate the buckling load possibly because the assumed four term expression for radial displacement function is inadequate.

2. CONCLUSIONS

The objective of this study was to investigate the initial postbuckling behavior and the imperfection sensitivity of composite cylindrical shells subjected to axial load by using Koiter's theory.

It is assumed that the prebuckling behavior is linear and that the shell is subjected to proportional loading. From the numerical results presented the following conclusions can be made:

1) The coefficient"b" is greater for glass-epoxy shells than for boron-epoxy shells. This suggests that the boron-epoxy shells are less imperfection sensitive than glass-epoxy shells.

2) The slope of the initial postbuckling curve depends upon the fiber orientation for boron-epoxy shells. However, for glass-epoxy shells the slope remains practically unchanged.

3) A significant increase in the classical buckling load can be achieved by proper change in fiber orientation. A shell with an efficient arrangement of fiber orientation with greater classical buckling load will be highly imperfection sensitive.

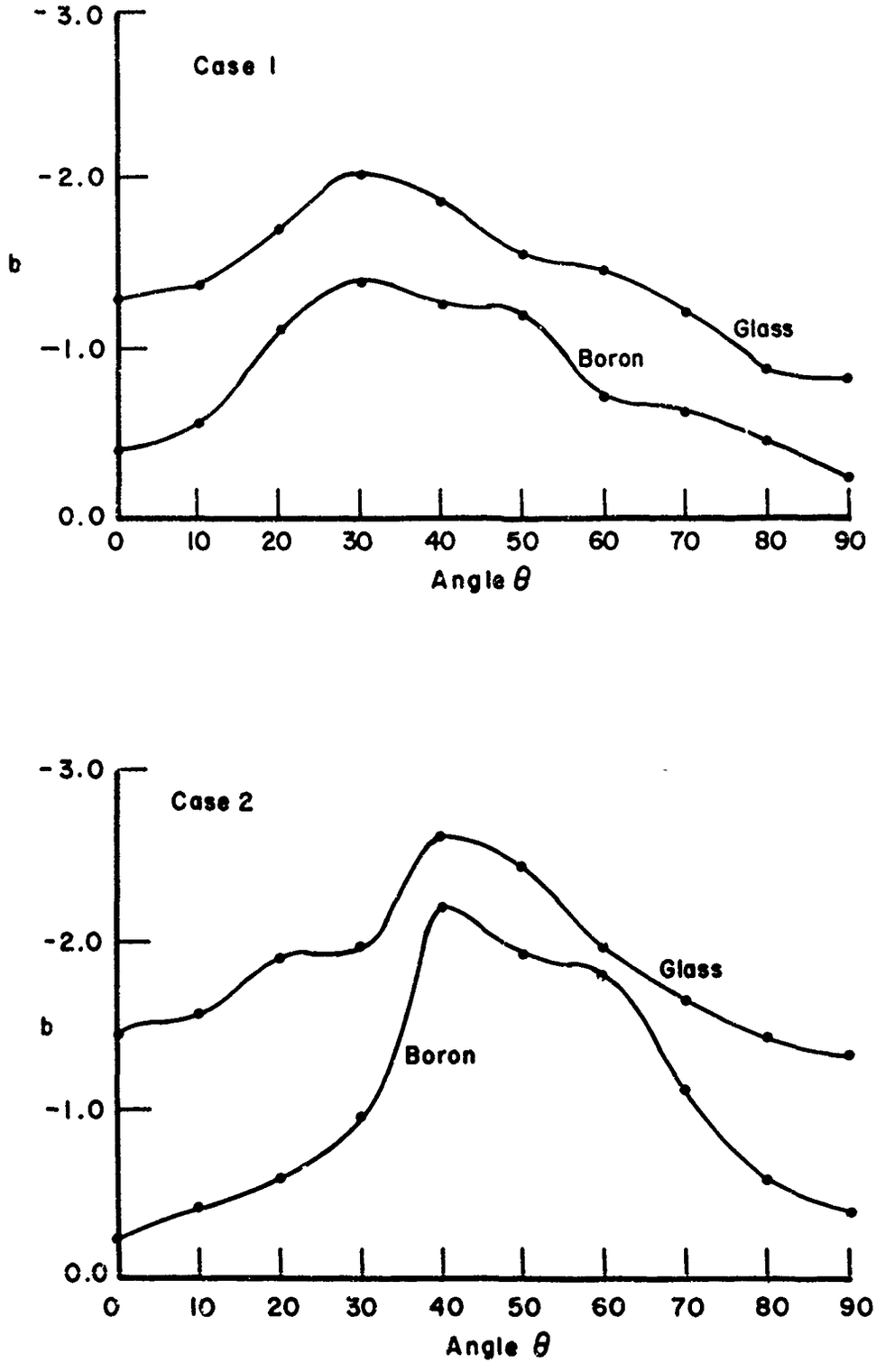

Figure 3. Effect of Fiber Orientation on the Coefficient b

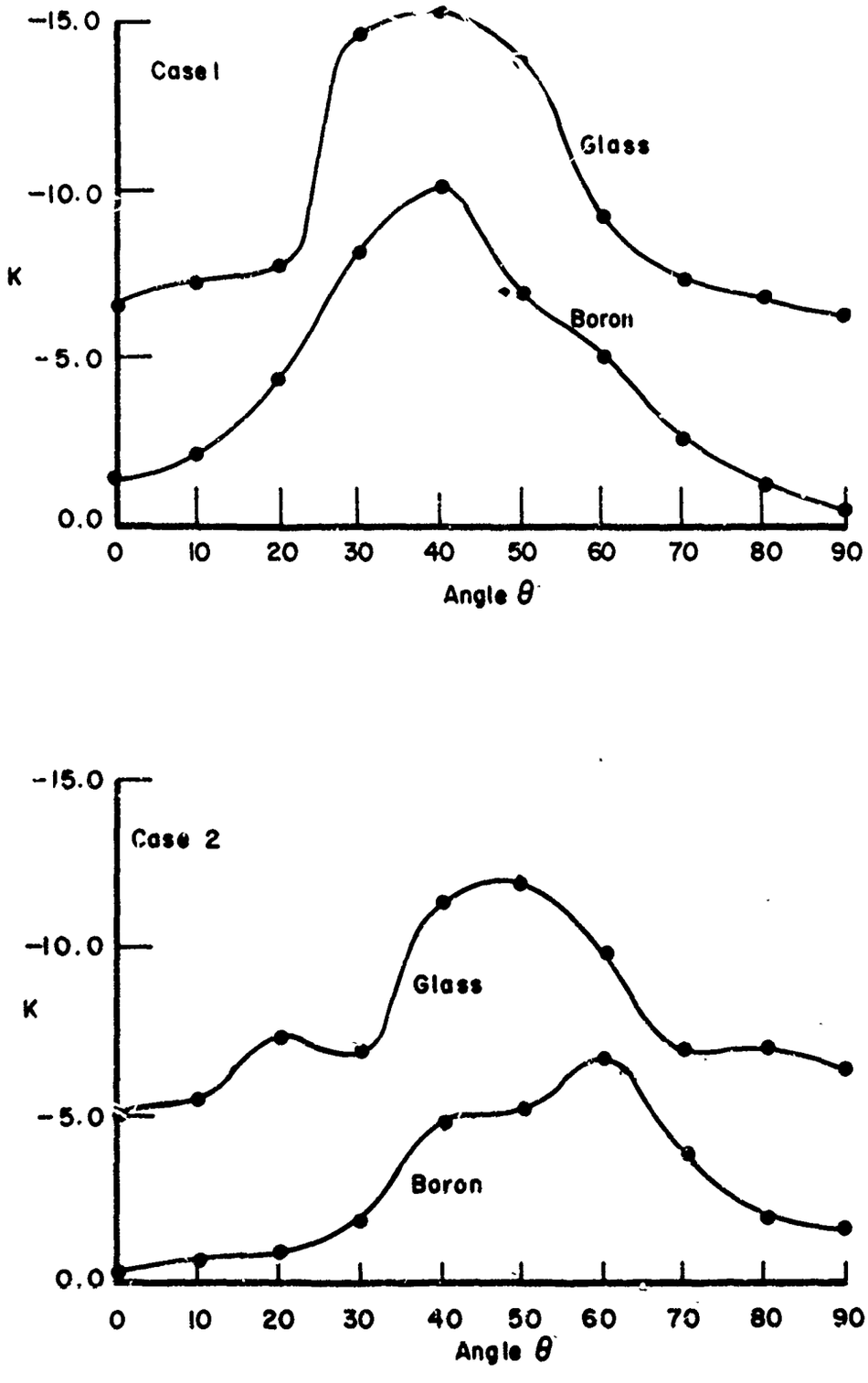

Figure 4. Effect of Fiber Orientation on the Coefficient K

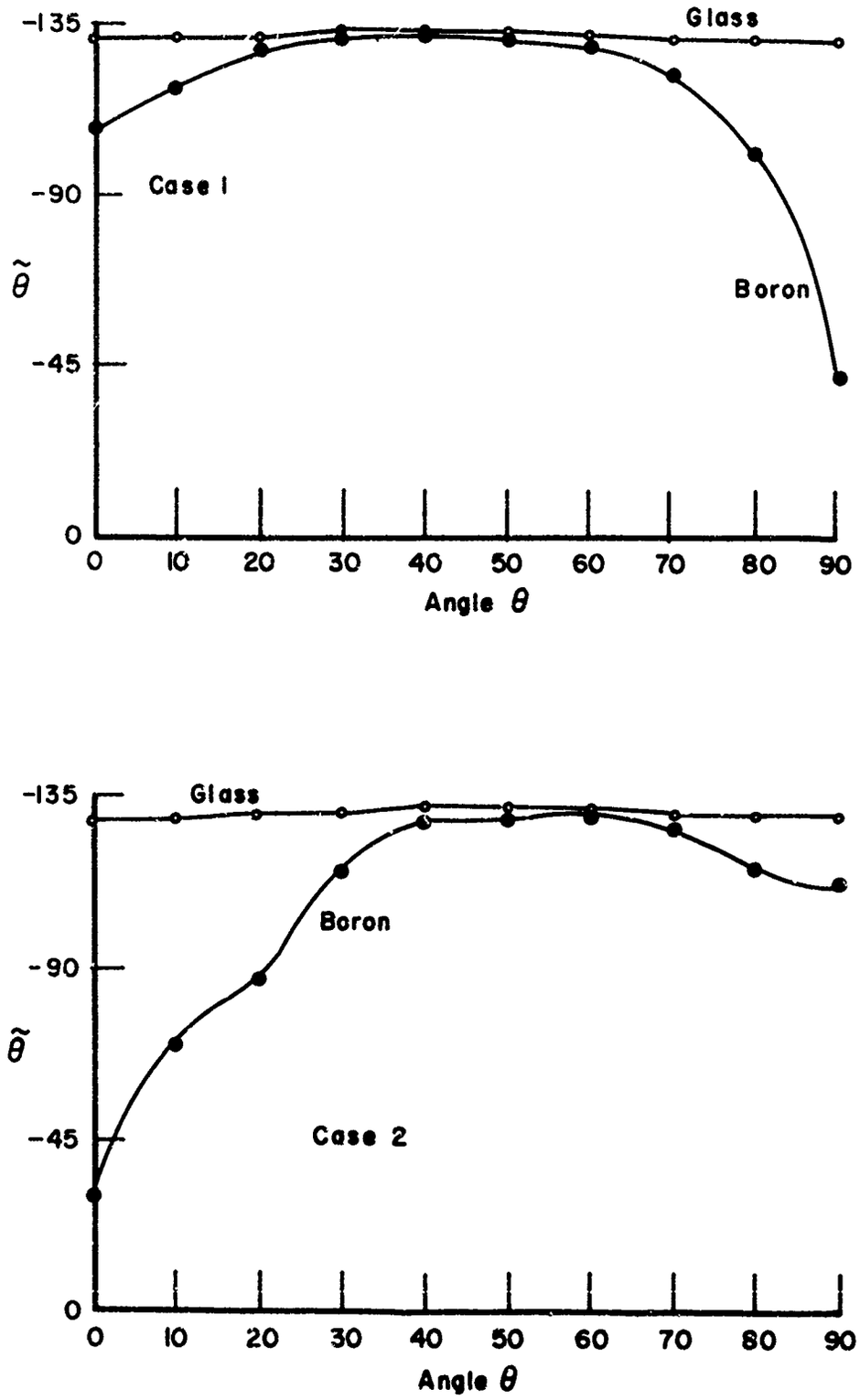

Figure 5. Effect of Fiber Orientation on the Angle $\tilde{\theta}$

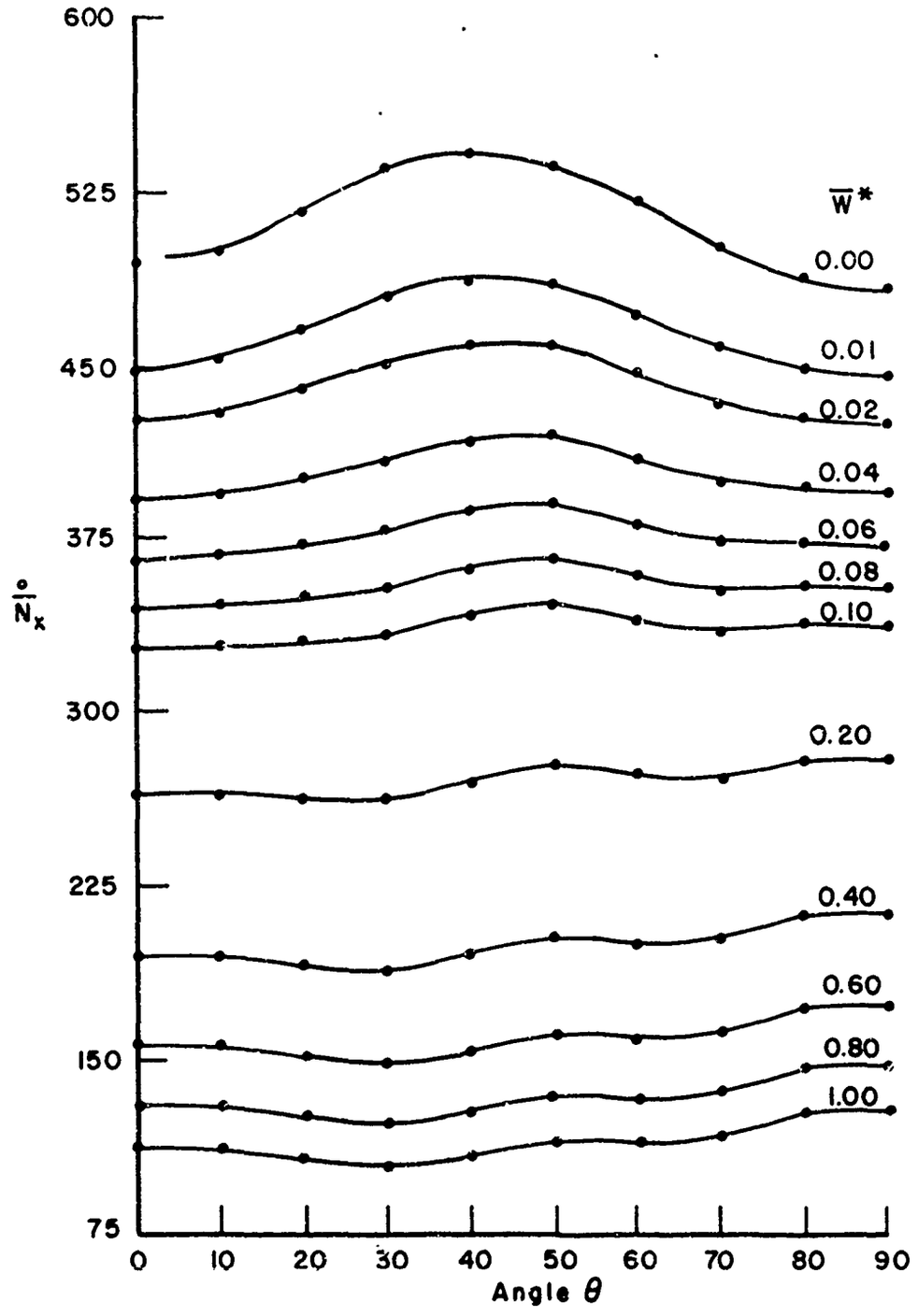

Figure 6. Influence of Initial Imperfection on Buckling Load of Glass-Epoxy Composite Cylinder for Case 1 (θ°,-θ°,0°)

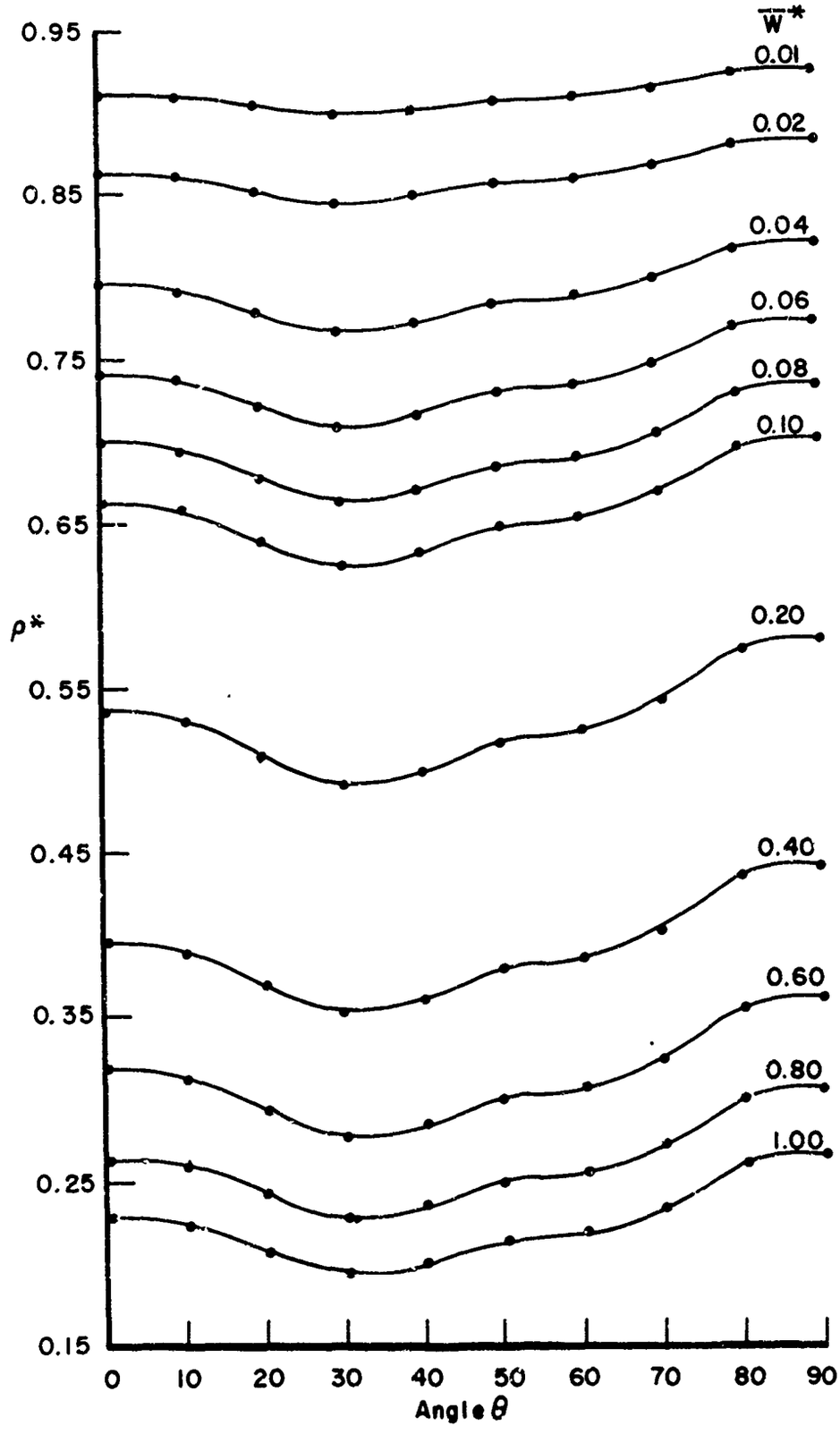

Figure 7. Imperfection Sensitivity of Glass-Epoxy Composite Cylinder for Case 1 ($\theta°$,-$\theta°$, 0°)

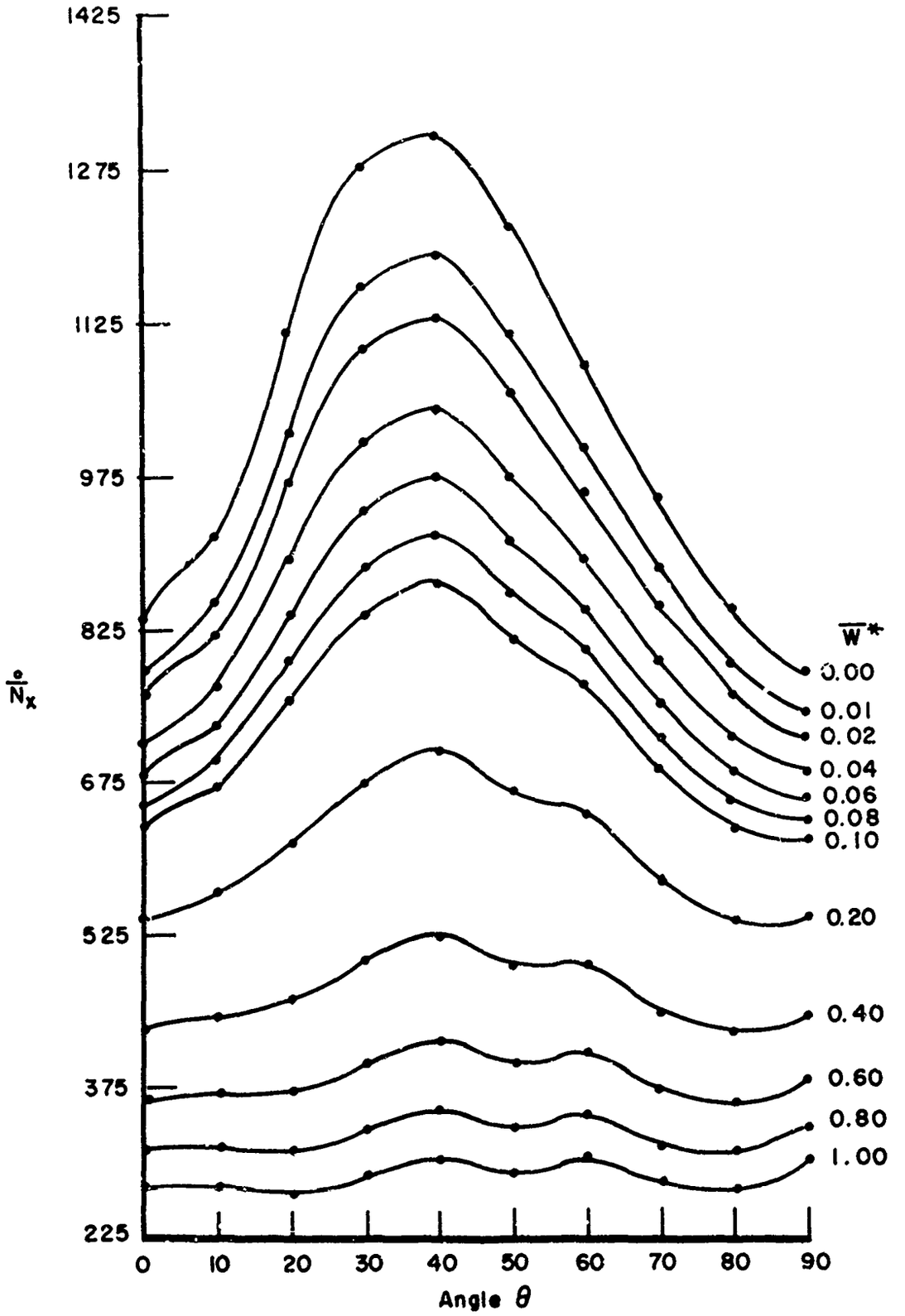

Figure 8. Influence of Initial Imperfection on Buckling Load of Boron-Epoxy Composite Cylinder for Case 1 ($\theta^\circ, -\theta^\circ, 0^\circ$)

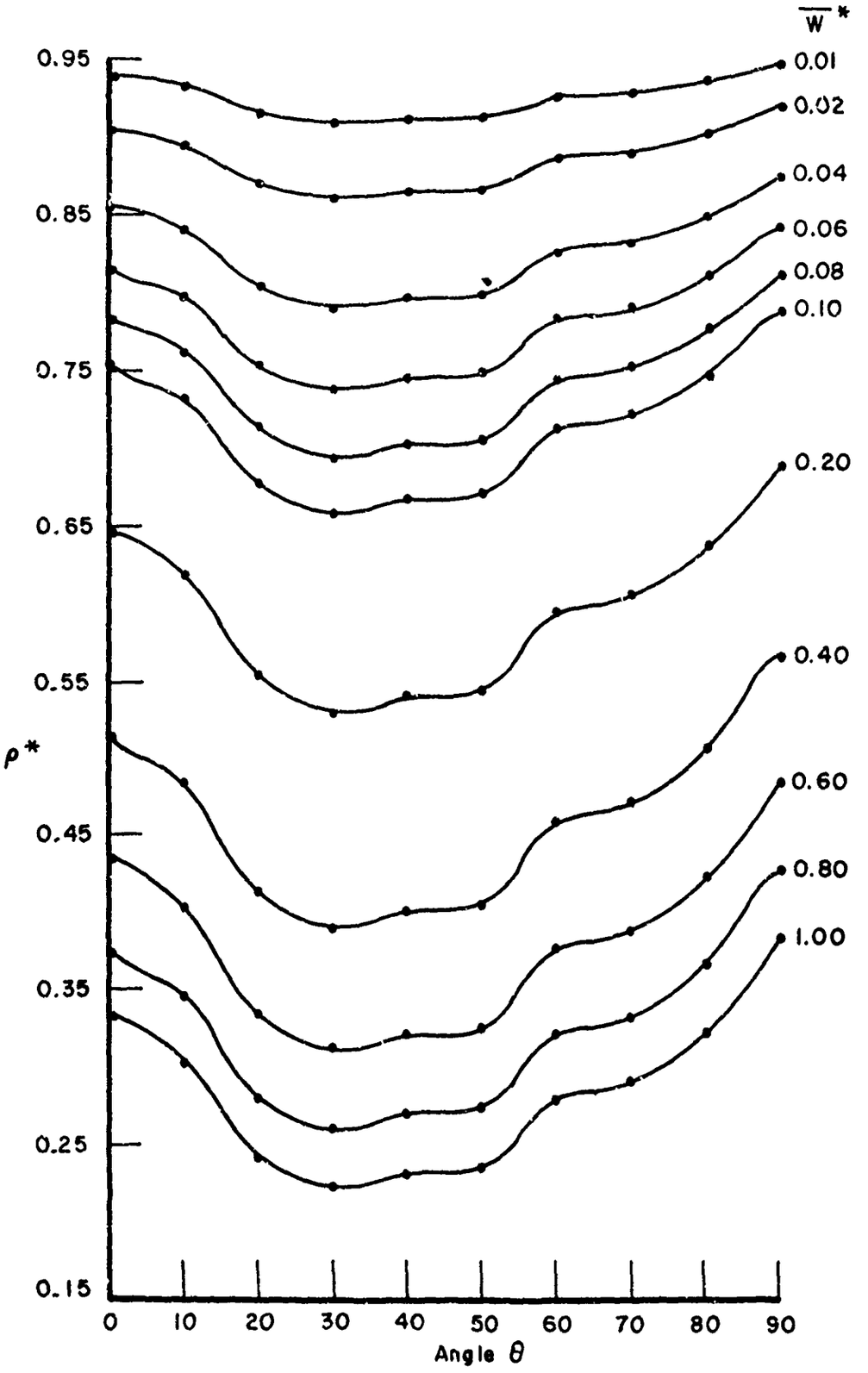

Figure 9. Imperfection Sensitivity of Boron-Epoxy Composite Cylinder for Case 1 $(\theta^\circ, -\theta^\circ, 0^\circ)$

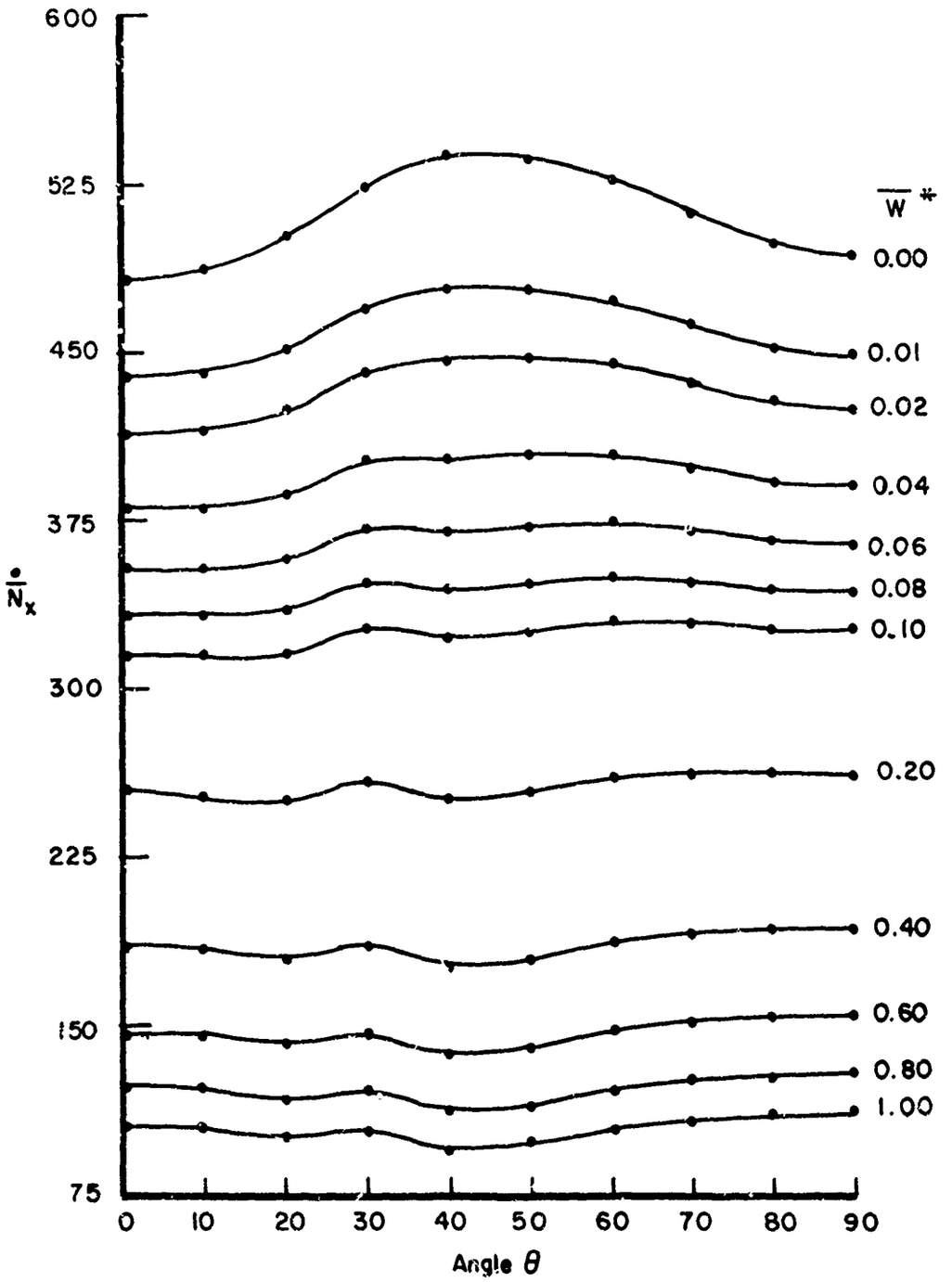

Figure 10. Influence of Initial Imperfection on Buckling Load of Glass-Epoxy Composite Cylinder for Case 2 $(\theta^\circ, -\theta^\circ, 90^\circ)$

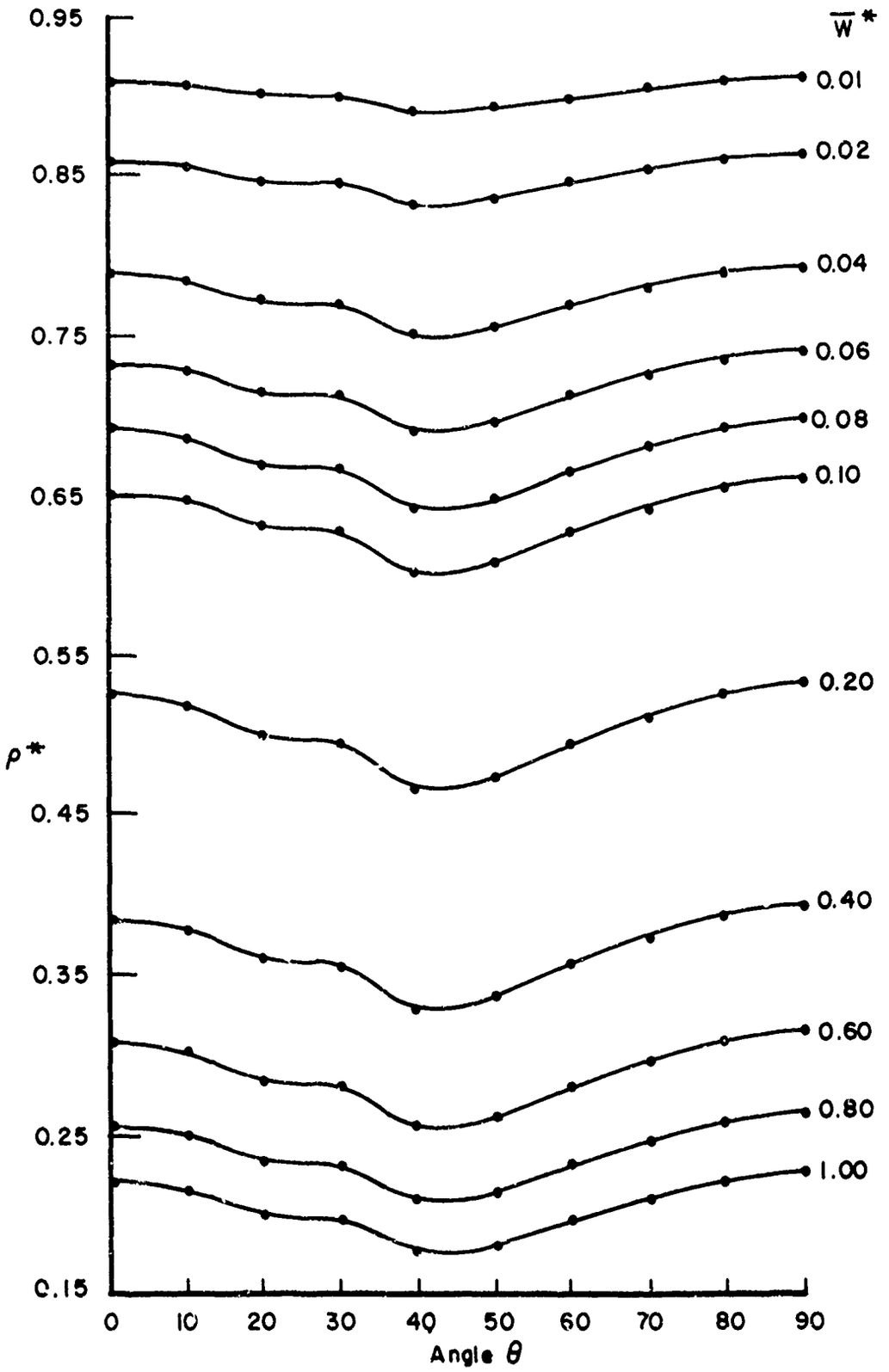

Figure 11. Imperfection Sensitivity of Glass-Epoxy Composite Cylinder for Case 2 ($\theta°, -\theta°, 90°$)

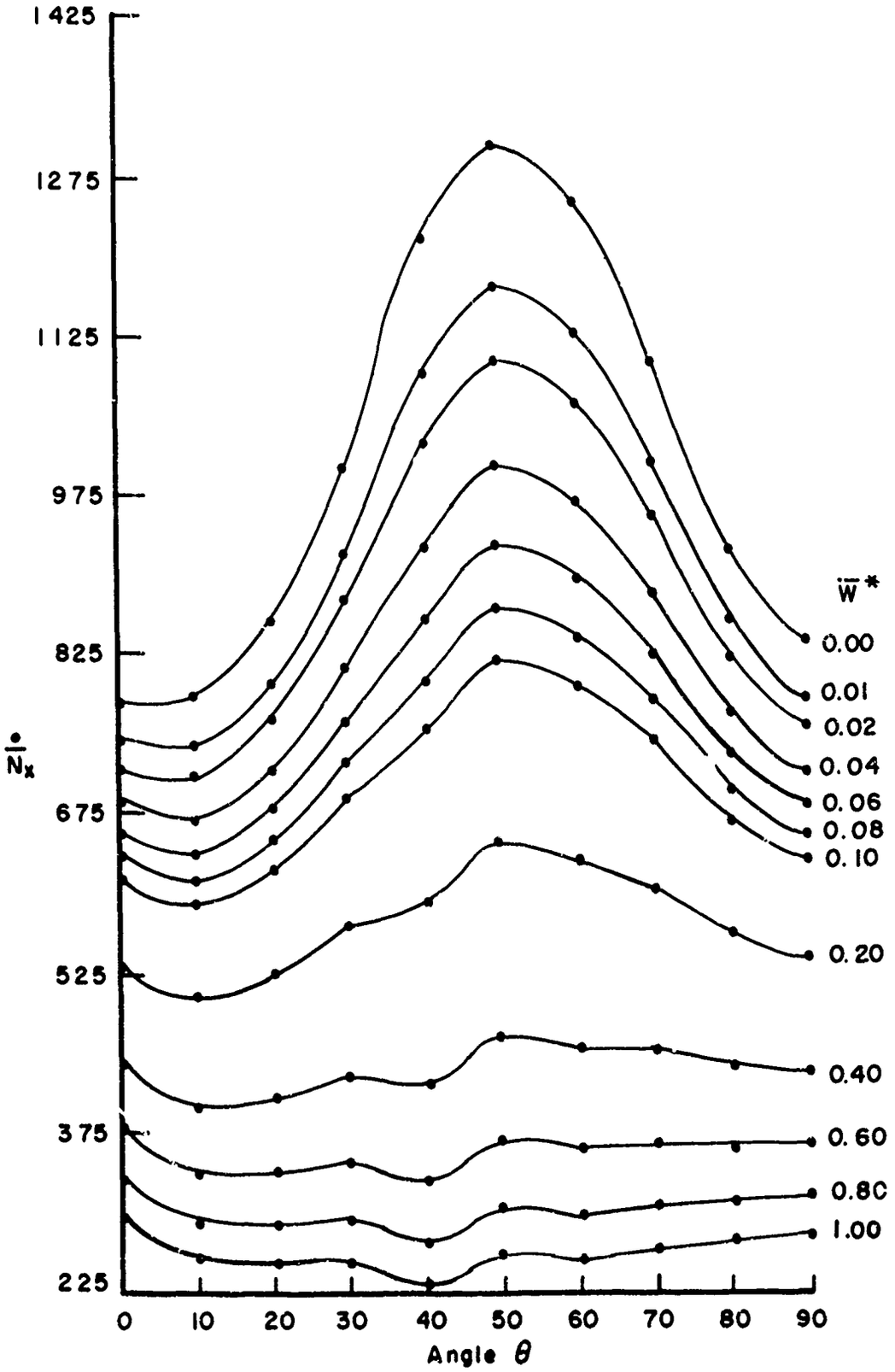

Figure 12. Influence of Initial Imperfection on Buckling Load of Boron-Epoxy Composite Cylinder for Case 2 ($\theta°$,-$\theta°$,90°)

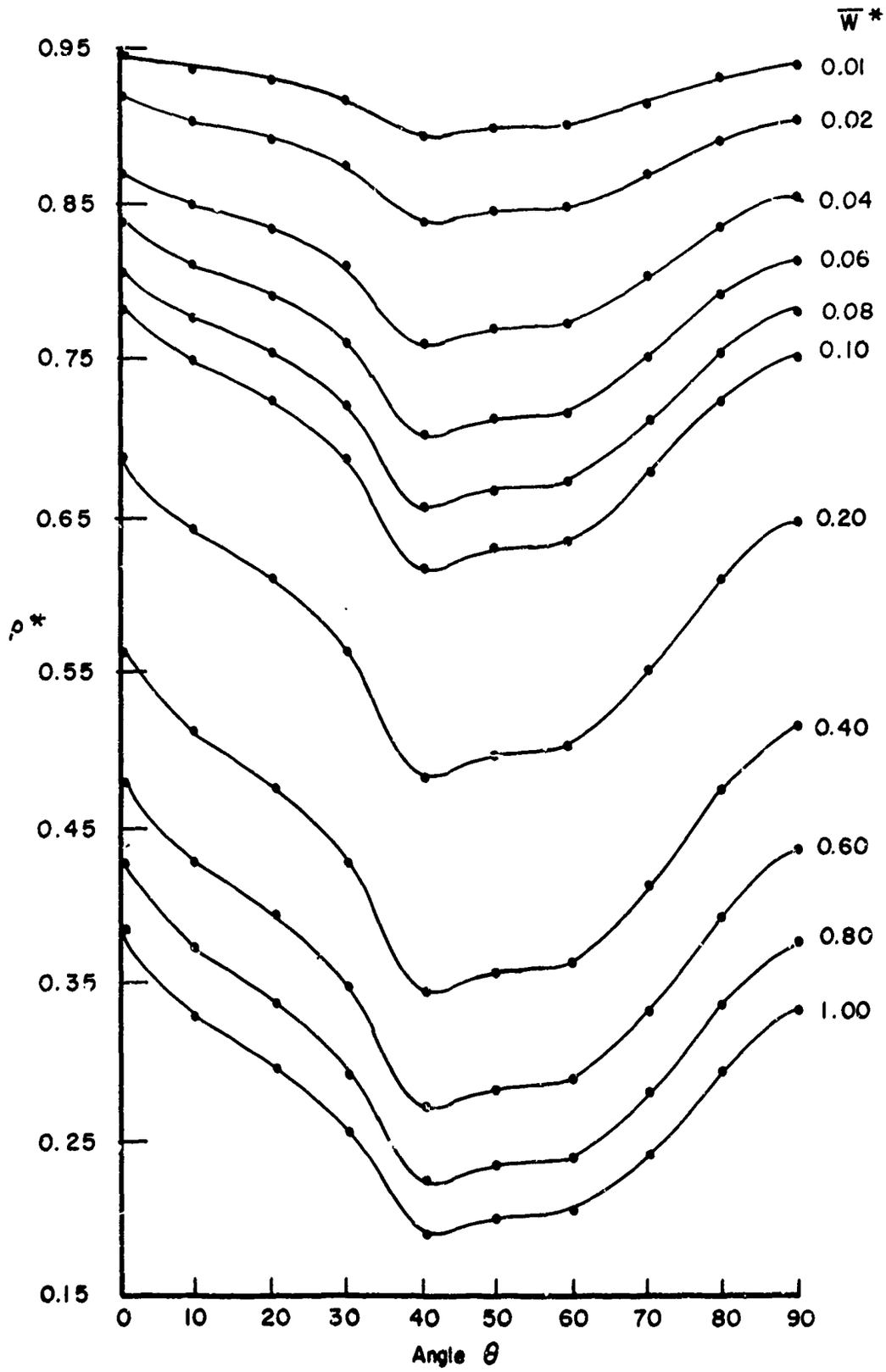

Figure 13. Imperfection Sensitivity of Boron-Epoxy Composite Cylinder for Case 2 ($\theta^\circ, -\theta^\circ, 90^\circ$)

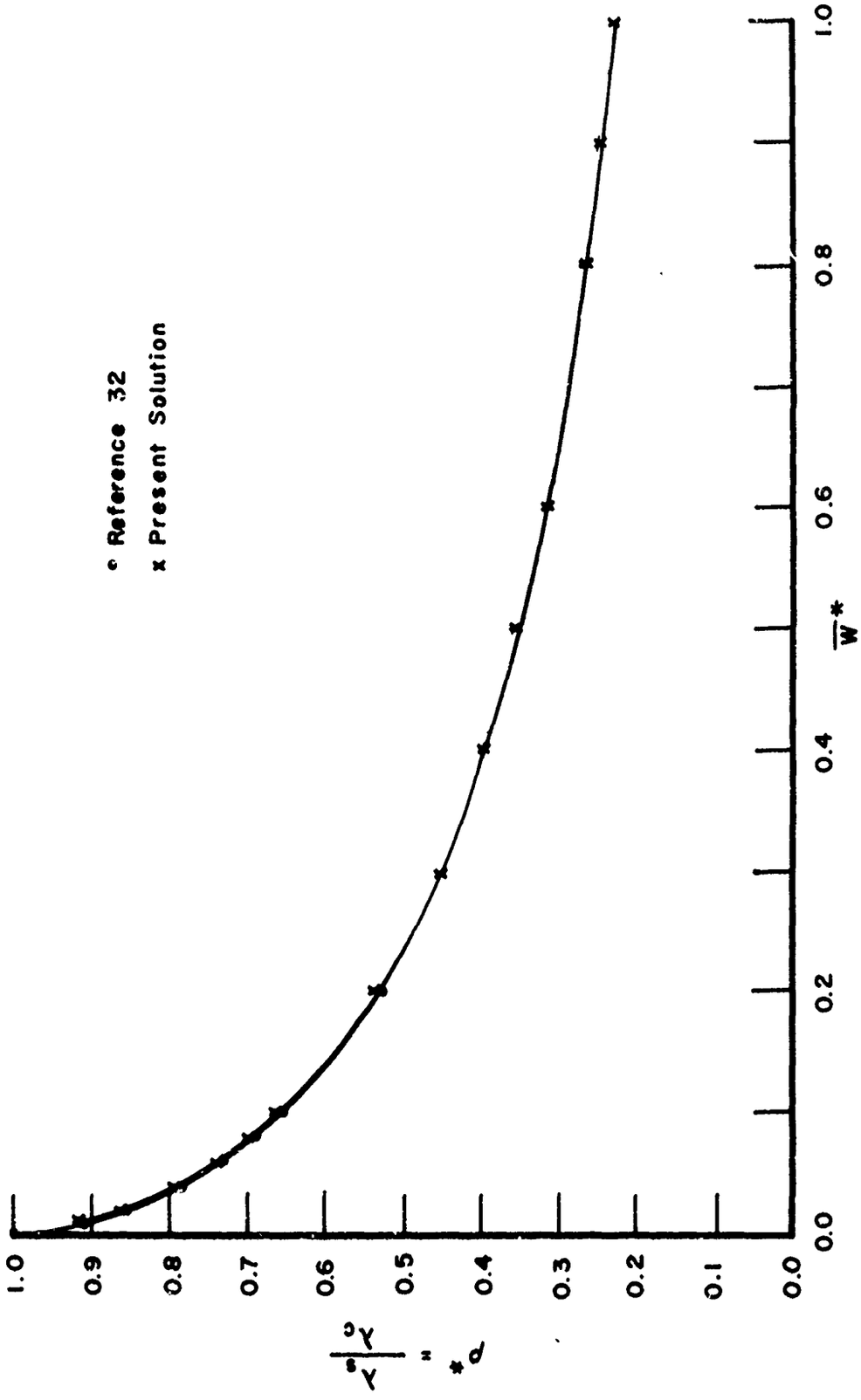

Figure 14. Effect of Imperfection on Axial Buckling Load for Glass-Epoxy Cylinder for Fiber Orientation (0°,0°,0°)

APPENDIX I

RESULTS FOR GLASS-EPOXY CYLINDRICAL SHELL

TABLE I-1

CLASSICAL BUCKLING LOADS FOR GLASS-EPOXY COMPOSITE CYLINDRICAL SHELL

CASE	$\overline{N}_x$	$\frac{\circ}{N_x}$	τ	m	n
1.00	7.5952E-01	4.9252E 02	0.	6	11
1.10	7.8169E-01	4.9917E 02	-8.5319E-02	6	11
1.20	8.4339E-01	5.1645E 02	-6.2068E-03	7	12
1.30	9.2195E-01	5.3473E 02	8.2758E-02	6	12
1.40	9.7402E-01	5.4200E 02	1.2210E-01	6	12
1.50	9.7010E-01	5.3668E 02	9.0924E-02	6	12
1.60	9.1464E-01	5.2119E 02	1.0179E-01	7	12
1.70	8.4149E-01	5.0247E 02	4.8323E-02	7	12
1.80	7.8230E-01	4.8752E 02	-1.3905E-03	6	11
1.90	7.6128E-01	4.8296E 02	0.	6	11
2.00	6.8953E-01	4.8169E 02	0.	8	11
2.10	7.0855E-01	4.8596E 02	-1.8861E-01	8	11
2.20	7.6841E-01	5.0081E 02	-3.1409E-01	8	11
2.30	8.5791E-01	5.2224E 02	-7.0748E-03	10	12
2.40	9.3295E-01	5.3689E 02	1.6057E-01	10	12
2.50	9.4474E-01	5.3569E 02	4.6953E-01	9	11
2.60	9.0268E-01	5.2638E 02	4.0416E-01	9	11
2.70	8.3732E-01	5.1198E 02	1.6398E-01	10	12
2.80	7.8123E-01	4.9811E 02	1.3703E-01	9	11
2.90	7.5961E-01	4.9258E 02	0.	9	11

TABLE I-2

COEFFICIENTS FOR INITIAL POSTBUCKLING BEHAVIOR OF GLASS-EPOXY COMPOSITE CYLINDRICAL SHELLS

CASE	b	K	1/K	$\bar{\theta}$
1.0	-1.2858E 00	-6.5494E 00	-1.5269E-01	-1.3028E 02
1.10	-1.3683E 00	-7.2222E 00	-1.3846E-01	-1.3075E 02
1.20	-1.6997E 00	-7.7070E 00	-1.2975E-01	-1.3103E 02
1.30	-2.0272E 00	-1.4573E 01	-6.8618E-02	-1.3297E 02
1.40	-1.8685E 00	-1.5319E 01	-6.5277E-02	-1.3307E 02
1.50	-1.5608E 00	-1.3816E 01	-7.2382E-02	-1.3285E 02
1.60	-1.4600E 00	-9.2855E 00	-1.0769E-01	-1.3174E 02
1.70	-1.2168E 00	-7.3407E 00	-1.3623E-01	-1.3082E 02
1.80	-8.7801E-01	-6.8650E 00	-1.4567E-01	-1.3051E 02
1.90	-8.2554E-01	-6.3296E 00	-1.5799E-01	-1.3010E 02
2.0	-1.4411E 00	-4.9801E 00	-2.0080E-01	-1.2863E 02
2.10	-1.5548E 00	-5.4624E 00	-1.8307E-01	-1.2925E 02
2.20	-1.8957E 00	-7.2920E 00	-1.3714E-01	-1.3079E 02
2.30	-1.9564E 00	-6.8003E 00	-1.4705E-01	-1.3046E 02
2.40	-2.6153E 00	-1.1257E 01	-8.8833E-02	-1.3234E 02
2.50	-2.4321E 00	-1.1888E 01	-8.4116E-02	-1.3249E 02
2.60	-1.9659E 00	-9.7792E 00	-1.0226E-01	-1.3192E 02
2.70	-1.6502E 00	-6.9205E 00	-1.4450E-01	-1.3055E 02
2.80	-1.4271E 00	-6.9444E 00	-1.4400E-01	-1.3056E 02
2.90	-1.3286E 00	-6.3947E 00	-1.5638E-01	-1.3015E 02

TABLE I-3

BUCKLING LOADS FOR IMPERFECT GLASS-EPOXY SHELL
$\bar{W}^* = 0.01$

CASE	$\bar{N}_x$	$\frac{\circ}{N_x}$	ρ^*
1.00	6.9147E-01	4.4839E 02	9.1040E-01
1.10	7.1027E-01	4.5357E 02	9.0864E-01
1.20	7.6095E-01	4.6597E 02	9.0225E-01
1.30	8.2677E-01	4.7952E 02	8.9676E-01
1.40	8.7597E-01	4.8744E 02	8.9933E-01
1.50	8.7776E-01	4.8559E 02	9.0481E-01
1.60	8.2937E-01	4.7260E 02	9.0677E-01
1.70	7.6738E-01	4.5822E 02	9.1193E-01
1.80	7.2012E-01	4.4877E 02	9.2051E-01
1.90	7.0193E-01	4.4531E 02	9.2204E-01
2.00	6.2551E-01	4.3696E 02	9.0715E-01
2.10	6.4118E-01	4.3976E 02	9.0492E-01
2.20	6.9071E-01	4.5017E 02	8.9888E-01
2.30	7.7031E-01	4.6891E 02	8.9789E-01
2.40	8.2876E-01	4.7693E 02	8.8832E-01
2.50	8.4156E-01	4.7719E 02	8.9079E-01
2.60	8.1037E-01	4.7255E 02	8.9774E-01
2.70	7.5622E-01	4.6239E 02	9.0315E-01
2.80	7.0891E-01	4.5200E 02	9.0743E-01
2.90	6.9085E-01	4.4799E 02	9.0948E-01

TABLE I-4

BUCKLING LOADS FOR IMPERFECT GLASS-EPOXY SHELL
$\overline{W}^* = 0.02$

CASE	$\overline{N}_x$	$\overline{N}_x^o$	ρ^*
1.0	6.5529E-01	4.2493E 02	8.6277E-01
1.10	6.7239E-01	4.2938E 02	8.6018E-01
1.20	7.1755E-01	4.3939E 02	8.5079E-01
1.30	7.7698E-01	4.5065E 02	8.4276E-01
1.40	8.2453E-01	4.5882E 02	8.4652E-01
1.50	8.2899E-01	4.5862E 02	8.5455E-01
1.60	7.8424E-01	4.4688E 02	8.5743E-01
1.70	7.2792E-01	4.3465E 02	8.6504E-01
1.80	6.8667E-01	4.2793E 02	8.7776E-01
1.90	6.6996E-01	4.2502E 02	8.8004E-01
2.0	5.9161E-01	4.1328E 02	8.5798E-01
2.10	6.0561E-01	4.1536E 02	8.5471E-01
2.20	6.4997E-01	4.2362E 02	8.4586E-01
2.30	7.2443E-01	4.4099E 02	8.4441E-01
2.40	7.7481E-01	4.4588E 02	8.3049E-01
2.50	7.8798E-01	4.4680E 02	8.3407E-01
2.60	7.6203E-01	4.4436E 02	8.4419E-01
2.70	7.1348E-01	4.3626E 02	8.5210E-01
2.80	6.7061E-01	4.2758E 02	8.5840E-01
2.90	6.5434E-01	4.2431E 02	8.6141E-01

TABLE I-5

BUCKLING LOADS FOR IMPERFECT GLASS-EPOXY SHELL
$\overline{W}^* = 0.04$

CASE	$\overline{N}_x$	$\dot{\overline{N}}_x$	ρ^*
1. C	6.0299E-01	3.9102E 02	7.9391E-01
1.10	6.1773E-01	3.9447E 02	7.9025E-01
1.20	6.5535E-01	4.0130E 02	7.7704E-01
1.30	7.0606E-01	4.0951E 02	7.6583E-01
1.40	7.5104E-01	4.1792E 02	7.7107E-01
1.50	7.5692E-01	4.1985E 02	7.8231E-01
1.60	7.1924E-01	4.0985E 02	7.8636E-01
1.70	6.7077E-01	4.0053E 02	7.9712E-01
1.80	6.3779E-01	3.9747E 02	8.1528E-01
1.90	6.2315E-01	3.9533E 02	8.1855E-01
2. C	5.4276E-01	3.7916E 02	7.8715E-01
2.10	5.5447E-01	3.8028E 02	7.8254E-01
2.20	5.9179E-01	3.8570E 02	7.7015E-01
2.30	6.5898E-01	4.0115E 02	7.6813E-01
2.40	6.9865E-01	4.0206E 02	7.4886E-01
2.50	7.1214E-01	4.0380E 02	7.5379E-01
2.60	6.9309E-01	4.0416E 02	7.6782E-01
2.70	6.5217E-01	3.9877E 02	7.7888E-01
2.80	6.1540E-01	3.9238E 02	7.8773E-01
2.90	6.0160E-01	3.9012E 02	7.9199E-01

TABLE I-6

BUCKLING LOADS FOR IMPERFECT GLASS-EPOXY SHELL
$\overline{W}^* = 0.06$

CASE	$\overline{N}_x$	$\dot{\overline{N}}_x$	ρ^*
1. 0	5.6347E-01	3.6539E 02	7.4188E-01
1.10	5.7651E-01	3.6814E 02	7.3751E-01
1.20	6.0880E-01	3.7280E 02	7.2184E-01
1.30	6.5332E-01	3.7893E 02	7.0863E-01
1.40	6.9623E-01	3.8742E 02	7.1480E-01
1.50	7.0631E-01	3.9075E 02	7.2808E-01
1.60	6.7034E-01	3.8198E 02	7.3290E-01
1.70	6.2751E-01	3.7470E 02	7.4571E-01
1.80	6.0042E-01	3.7417E 02	7.6750E-01
1.90	5.8729E-01	3.7258E 02	7.7145E-01
2. 0	5.0600E-01	3.5348E 02	7.3383E-01
2.10	5.1608E-01	3.5395E 02	7.2836E-01
2.20	5.4842E-01	3.5743E 02	7.1371E-01
2.30	6.1026E-01	3.7148E 02	7.1133E-01
2.40	6.4258E-01	3.6979E 02	6.8876E-01
2.50	6.5614E-01	3.7205E 02	6.9452E-01
2.60	6.4177E-01	3.7424E 02	7.1096E-01
2.70	6.0623E-01	3.7068E 02	7.2402E-01
2.80	5.7383E-01	3.6587E 02	7.3452E-01
2.90	5.6180E-01	3.6431E 02	7.3959E-01

TABLE I-6

BUCKLING LOADS FOR IMPERFECT GLASS-EPOXY SHELL
$\overline{W}^* = 0.06$

CASE	$\overline{N}_x$	$\overset{\bullet}{\overline{N}}_x$	ρ^*
1. 0	5.6347E-01	3.6539E 02	7.4188E-01
1.10	5.7651E-01	3.6814E 02	7.3751E-01
1.20	6.0880E-01	3.7280E 02	7.2184E-01
1.30	6.5332E-01	3.7893E 02	7.0863E-01
1.40	6.9623E-01	3.8742E 02	7.1480E-01
1.50	7.0631E-01	3.9075E 02	7.2808E-01
1.60	6.7034E-01	3.8198E 02	7.3290E-01
1.70	6.2751E-01	3.7470E 02	7.4571E-01
1.80	6.0042E-01	3.7417E 02	7.6750E-01
1.90	5.8729E-01	3.7258E 02	7.7145E-01
2. 0	5.0600E-01	3.5348E 02	7.3383E-01
2.10	5.1608E-01	3.5395E 02	7.2836E-01
2.20	5.4842E-01	3.5743E 02	7.1371E-01
2.30	6.1026E-01	3.7148E 02	7.1133E-01
2.40	6.4258E-01	3.6979E 02	6.8876E-01
2.50	6.5614E-01	3.7205E 02	6.9452E-01
2.60	6.4177E-01	3.7424E 02	7.1096E-01
2.70	6.0623E-01	3.7068E 02	7.2402E-01
2.80	5.7383E-01	3.6587E 02	7.3452E-01
2.90	5.6180E-01	3.6431E 02	7.3959E-01

TABLE I-8

BUCKLING LOADS FOR IMPERFECT GLASS-EPOXY SHELL
$\overline{W}^* = 0.10$

CASE	$\overline{N}_x$	$\frac{o}{N}_x$	ρ^*
1. 0	5.0376E-01	3.2667E 02	6.6327E-01
1.10	5.1437E-01	3.2847E 02	6.5803E-01
1.20	5.3924E-01	3.3020E 02	6.3937E-01
1.30	5.7511E-01	3.3356E 02	6.2379E-01
1.40	6.1465E-01	3.4203E 02	6.3105E-01
1.50	6.2744E-01	3.4711E 02	6.4677E-01
1.60	5.9681E-01	3.4008E 02	6.5251E-01
1.70	5.6201E-01	3.3559E 02	6.6787E-01
1.80	5.4315E-01	3.3848E 02	6.9430E-01
1.90	5.3223E-01	3.3765E 02	6.9913E-01
2. 0	4.5069E-01	3.1484E 02	6.5362E-01
2.10	4.5851E-01	3.1447E 02	6.4711E-01
2.20	4.8392E-01	3.1539E 02	6.2977E-01
2.30	5.3788E-01	3.2743E 02	6.2697E-01
2.40	5.6037E-01	3.2248E 02	6.0065E-01
2.50	5.7376E-01	3.2533E 02	6.0732E-01
2.60	5.6556E-01	3.2979E 02	6.2653E-01
2.70	5.3752E-01	3.2866E 02	6.4195E-01
2.80	5.1128E-01	3.2599E 02	6.5445E-01
2.90	5.0173E-01	3.2536E 02	6.6051E-01

TABLE I-9

BUCKLING LOADS FOR IMPERFECT GLASS-EPOXY SHELL
$\overline{W}^* = 0.20$

CASE	$\overline{N}_x$	$\mathring{N}_x$	ρ^*
1.0	4.0722E-01	2.6407E 02	5.3616E-01
1.10	4.1433E-01	2.6458E 02	5.3004E-01
1.20	4.2891E-01	2.6264E 02	5.0856E-01
1.30	4.5262E-01	2.6252E 02	4.9094E-01
1.40	4.8614E-01	2.7051E 02	4.9910E-01
1.50	5.0157E-01	2.7748E 02	5.1703E-01
1.60	4.7895E-01	2.7292E 02	5.2365E-01
1.70	4.5571E-01	2.7211E 02	5.4155E-01
1.80	4.4828E-01	2.7936E 02	5.7302E-01
1.90	4.4068E-01	2.7957E 02	5.7887E-01
2.0	3.6196E-01	2.5285E 02	5.2493E-01
2.10	3.6662E-01	2.5144E 02	5.1742E-01
2.20	3.8241E-01	2.4923E 02	4.9766E-01
2.30	4.2424E-01	2.5825E 02	4.9450E-01
2.40	4.3410E-01	2.4981E 02	4.6530E-01
2.50	4.4650E-01	2.5318E 02	4.7262E-01
2.60	4.4594E-01	2.6004E 02	4.9402E-01
2.70	4.2829E-01	2.6188E 02	5.1150E-01
2.80	4.1085E-01	2.6195E 02	5.2590E-01
2.90	4.0483E-01	2.6252E 02	5.3294E-01

TABLE I-10

BUCKLING LOADS FOR IMPERFECT GLASS-EPOXY SHELL
$\overline{W}^* = 0.30$

CASE	$\overline{N}_x$	$\overline{N}_x^\circ$	ρ^*
1. 0	3.4566E-01	2.2415E 02	4.5510E-01
1.10	3.5084E-01	2.2404E 02	4.4882E-01
1.20	3.6007E-01	2.2049E 02	4.2693E-01
1.30	3.7726E-01	2.1881E 02	4.0920E-01
1.40	4.0655E-01	2.2623E 02	4.1739E-01
1.50	4.2251E-01	2.3374E 02	4.3553E-01
1.60	4.0452E-01	2.3051E 02	4.4227E-01
1.70	3.8765E-01	2.3148E 02	4.6067E-01
1.80	3.8609E-01	2.4060E 02	4.9353E-01
1.90	3.8041E-01	2.4133E 02	4.9970E-01
2. 0	3.0587E-01	2.1367E 02	4.4359E-01
2.10	3.0887E-01	2.1184E 02	4.3592E-01
2.20	3.1961E-01	2.0831E 02	4.1594E-01
2.30	3.5412E-01	2.1557E 02	4.1277E-01
2.40	3.5804E-01	2.0604E 02	3.8377E-01
2.50	3.6939E-01	2.0945E 02	3.9099E-01
2.60	3.7216E-01	2.1702E 02	4.1228E-01
2.70	3.5997E-01	2.2010E 02	4.2991E-01
2.80	3.4731E-01	2.2145E 02	4.4457E-01
2.90	3.4319E-01	2.2255E 02	4.5180E-01

TABLE I-11

BUCKLING LOADS FOR IMPERFECT GLASS-EPOXY SHELL
$\overline{W}^* = 0.40$

CASE	$\overline{N}_x$	$\overset{\circ}{N}_x$	ρ^*
1.00	3.0166E-01	1.9562E 02	3.9718E-01
1.10	3.0562E-01	1.9516E 02	3.9098E-01
1.20	3.1164E-01	1.9083E 02	3.6951E-01
1.30	3.2480E-01	1.8838E 02	3.5229E-01
1.40	3.5087E-01	1.9524E 02	3.6023E-01
1.50	3.6661E-01	2.0282E 02	3.7791E-01
1.60	3.5170E-01	2.0041E 02	3.8453E-01
1.70	3.3886E-01	2.0234E 02	4.0269E-01
1.80	3.4071E-01	2.1233E 02	4.3552E-01
1.90	3.3629E-01	2.1334E 02	4.4174E-01
2.00	2.6603E-01	1.8585E 02	3.8582E-01
2.10	2.6804E-01	1.8384E 02	3.7829E-01
2.20	2.7572E-01	1.7970E 02	3.5882E-01
2.30	3.0520E-01	1.8579E 02	3.5575E-01
2.40	3.0589E-01	1.7603E 02	3.2787E-01
2.50	3.1627E-01	1.7933E 02	3.3477E-01
2.60	3.2070E-01	1.8701E 02	3.5528E-01
2.70	3.1183E-01	1.9067E 02	3.7242E-01
2.80	3.0217E-01	1.9266E 02	3.8679E-01
2.90	2.9922E-01	1.9403E 02	3.9391E-01

TABLE 1-12

BUCKLING LOADS FOR IMPERFECT GLASS-EPOXY SHELL
$\overline{W}^* = 0.50$

CASE	$\overline{N}_x$	$\overline{N}_x^o$	ρ^*
1.00	2.6824E-01	1.7394E 02	3.5317E-01
1.10	2.7136E-01	1.7328E 02	3.4715E-01
1.20	2.7530E-01	1.6858E 02	3.2642E-01
1.30	2.8574E-01	1.6573E 02	3.0993E-01
1.40	3.0927E-01	1.7209E 02	3.1752E-01
1.50	3.2451E-01	1.7953E 02	3.3451E-01
1.60	3.1180E-01	1.7767E 02	3.4090E-01
1.70	3.0170E-01	1.8015E 02	3.5853E-01
1.80	3.0566E-01	1.9048E 02	3.9071E-01
1.90	3.0212E-01	1.9167E 02	3.9686E-01
2.00	2.3592E-01	1.6481E 02	3.4215E-01
2.10	2.3728E-01	1.6274E 02	3.3488E-01
2.20	2.4295E-01	1.5834E 02	3.1617E-01
2.30	2.6872E-01	1.6358E 02	3.1323E-01
2.40	2.6751E-01	1.5395E 02	2.8674E-01
2.50	2.7706E-01	1.5710E 02	2.9327E-01
2.60	2.8234E-01	1.6464E 02	3.1278E-01
2.70	2.7566E-01	1.6855E 02	3.2922E-01
2.80	2.6803E-01	1.7090E 02	3.4309E-01
2.90	2.6586E-01	1.7240E 02	3.4999E-01

TABLE I-13

BUCKLING LOADS FOR IMPERFECT GLASS-EPOXY SHELL
$\overline{W}^* = 0.80$

CASE	$\overline{N}_x$	$\dot{\overline{N}}_x$	ρ^*
1. 0	2.0243E-01	1.3127E 02	2.6653E-01
1.10	2.0417E-01	1.3038E 02	2.6119E-01
1.20	2.0498E-01	1.2552E 02	2.4304E-01
1.30	2.1098E-01	1.2237E 02	2.2884E-01
1.40	2.2923E-01	1.2756E 02	2.3535E-01
1.50	2.4261E-01	1.3422E 02	2.5009E-01
1.60	2.3386E-01	1.3326E 02	2.5569E-01
1.70	2.2830E-01	1.3632E 02	2.7131E-01
1.80	2.3503E-01	1.4647E 02	3.0043E-01
1.90	2.3302E-01	1.4783E 02	3.0609E-01
2. 0	1.7706E-01	1.2369E 02	2.5679E-01
2.10	1.7743E-01	1.2169E 02	2.5041E-01
2.20	1.7995E-01	1.1728E 02	2.3419E-01
2.30	1.9875E-01	1.2098E 02	2.3166E-01
2.40	1.9518E-01	1.1232E 02	2.0921E-01
2.50	2.0283E-01	1.1501E 02	2.1470E-01
2.60	2.0877E-01	1.2174E 02	2.3128E-01
2.70	2.0554E-01	1.2568E 02	2.4547E-01
2.80	2.0126E-01	1.2832E 02	2.5762E-01
2.90	2.0032E-01	1.2990E 02	2.6371E-01

TABLE I-14

BUCKLING LOADS FOR IMPERFECT GLASS-EPOXY SHELL
$\overline{w}^* = 0.90$

CASE	$\overline{N}_x$	$\frac{\bullet}{N}_x$	ρ^*
1.0	1.8732E-01	1.2147E 02	2.4662E-01
1.10	1.8879E-01	1.2056E 02	2.4151E-01
1.20	1.6906E-01	1.1577E 02	2.2417E-01
1.30	1.9421E-01	1.1264E 02	2.1065E-01
1.40	2.1120E-01	1.1753E 02	2.1684E-01
1.50	2.2399E-01	1.2392E 02	2.3089E-01
1.60	2.1608E-01	1.2313E 02	2.3624E-01
1.70	2.1139E-01	1.2623E 02	2.5121E-01
1.80	2.1847E-01	1.3615E 02	2.7927E-01
1.90	2.1676E-01	1.3751E 02	2.8473E-01
2.0	1.6362E-01	1.1430E 02	2.3730E-01
2.10	1.6382E-01	1.1235E 02	2.3120E-01
2.20	1.6577E-01	1.0804E 02	2.1573E-01
2.30	1.8302E-01	1.1141E 02	2.1333E-01
2.40	1.7918E-01	1.0311E 02	1.9205E-01
2.50	1.8634E-01	1.0566E 02	1.9724E-01
2.60	1.9224E-01	1.1210E 02	2.1297E-01
2.70	1.8964E-01	1.1596E 02	2.2649E-01
2.80	1.8600E-01	1.1859E 02	2.3809E-01
2.90	1.8529E-01	1.2015E 02	2.4392E-01

TABLE I-15

BUCKLING LOADS FOR IMPERFECT GLASS-EPOXY SHELL
$\overline{W}^* = 1.00$

CASE	$\overline{N}_x$	$\dot{\overline{N}}_x$	ρ^*
1. 0	1.7435E-01	1.1306E 02	2.2955E-01
1.10	1.7561E-01	1.1214E 02	2.2465E-01
1.20	1.7548E-01	1.0745E 02	2.0806E-01
1.30	1.7995E-01	1.0437E 02	1.9518E-01
1.40	1.9585E-01	1.0898E 02	2.0108E-01
1.50	2.0808E-01	1.1511E 02	2.1449E-01
1.60	2.0086E-01	1.1446E 02	2.1961E-01
1.70	1.9687E-01	1.1755E 02	2.3395E-01
1.80	2.0416E-01	1.2723E 02	2.6097E-01
1.90	2.0269E-01	1.2859E 02	2.6625E-01
2. 0	1.5212E-01	1.0627E 02	2.2061E-01
2.10	1.5218E-01	1.0438E 02	2.1478E-01
2.20	1.5370E-01	1.0017E 02	2.0002E-01
2.30	1.6964E-01	1.0327E 02	1.9774E-01
2.40	1.6563E-01	9.5313E 01	1.7753E-01
2.50	1.7236E-01	9.7734E 01	1.8245E-01
2.60	1.7818E-01	1.0390E 02	1.9739E-01
2.70	1.7607E-01	1.0766E 02	2.1028E-01
2.80	1.7294E-01	1.1027E 02	2.2137E-01
2.90	1.7240E-01	1.1180E 02	2.2696E-01

TABLE I-16

BUCKLING LOADS FOR IMPERFECT GLASS-EPOXY SHELL
$\bar{W}^* = 1.10$

CASE	$\overline{N}_x$	$\dot{\overline{N}}_x$	ρ^*
1.00	1.6309E-01	1.0576E 02	2.1473E-01
1.10	1.6418E-01	1.0484E 02	2.1003E-01
1.20	1.6375E-01	1.0027E 02	1.9415E-01
1.30	1.6767E-01	9.7248E 01	1.8186E-01
1.40	1.8261E-01	1.0162E 02	1.8748E-01
1.50	1.9431E-01	1.0750E 02	2.0030E-01
1.60	1.8768E-01	1.0695E 02	2.0520E-01
1.70	1.8425E-01	1.1002E 02	2.1896E-01
1.80	1.9165E-01	1.1944E 02	2.4498E-01
1.90	1.9039E-01	1.2078E 02	2.5009E-01
2.00	1.4215E-01	9.9306E 01	2.0616E-01
2.10	1.4212E-01	9.7473E 01	2.0058E-01
2.20	1.4329E-01	9.3390E 01	1.8648E-01
2.30	1.5811E-01	9.6248E 01	1.8430E-01
2.40	1.5400E-01	8.8625E 01	1.6507E-01
2.50	1.6036E-01	9.0928E 01	1.6974E-01
2.60	1.6606E-01	9.6836E 01	1.8397E-01
2.70	1.6434E-01	1.0049E 02	1.9627E-01
2.80	1.6163E-01	1.0305E 02	2.0689E-01
2.90	1.6123E-01	1.0455E 02	2.1225E-01

TABLE I-17

BUCKLING LOADS FOR IMPERFECT GLASS-EPOXY SHELL
$\overline{W}^* = 1.20$

CASE	$\overline{N_x}$	$\dot{\overline{N}}_x$	ρ^*
1.0	1.5323E-01	9.9362E 01	2.0174E-01
1.10	1.5417E-01	9.8450E 01	1.9723E-01
1.20	1.5351E-01	9.4000E 01	1.8201E-01
1.30	1.5698E-01	9.1046E 01	1.7027E-01
1.40	1.7107E-01	9.5192E 01	1.7563E-01
1.50	1.8228E-01	1.0084E 02	1.8789E-01
1.60	1.7615E-01	1.0038E 02	1.9259E-01
1.70	1.7318E-01	1.0341E 02	2.0580E-01
1.80	1.8062E-01	1.1256E 02	2.3089E-01
1.90	1.7953E-01	1.1389E 02	2.3582E-01
2.0	1.3343E-01	9.3214E 01	1.9351E-01
2.10	1.3332E-01	9.1437E 01	1.8816E-01
2.20	1.3422E-01	8.7477E 01	1.7467E-01
2.30	1.4807E-01	9.0134E 01	1.7259E-01
2.40	1.4392E-01	8.2822E 01	1.5426E-01
2.50	1.4994E-01	8.5018E 01	1.5871E-01
2.60	1.5551E-01	9.0681E 01	1.7227E-01
2.70	1.5410E-01	9.4223E 01	1.8404E-01
2.80	1.5172E-01	9.6738E 01	1.9421E-01
2.90	1.5143E-01	9.8199E 01	1.9936E-01

APPENDIX II

RESULTS FOR BORON-EPOXY CYLINDRICAL SHELL

TABLE II-1

CLASSICAL BUCKLING LOADS FOR BORON-EPOXY COMPOSITE CYLINDRICAL SHELL

CASE	$\bar{N}_x$	$\dot{\bar{N}}_x$	τ	m	n
1.00	4.9689E-01	8.3431E 02	0.	4	10
1.10	5.5830E-01	9.1484E 02	-1.3180E-01	4	11
1.20	7.3189E-01	1.1139E 03	-3.6614E-02	5	12
1.30	9.2889E-01	1.2774E 03	1.5877E-01	5	13
1.40	1.0063E 00	1.3076E 03	9.9878E-02	5	13
1.50	9.1776E-01	1.2198E 03	3.5287E-02	6	13
1.60	7.5523E-01	1.0814E 03	-1.4138E-01	5	12
1.70	5.9751E-01	9.5176E 02	-2.1646E-01	6	12
1.80	4.5831E-01	8.4310E 02	-1.1822E-01	7	11
1.90	3.8187E-01	7.8051E 02	0.	8	11
2.00	3.6906E-01	7.8186E 02	0.	7	11
2.10	3.8304E-01	7.8503E 02	-4.6531E-01	6	10
2.20	4.6081E-01	8.5540E 02	-5.5227E-01	7	11
2.30	6.2866E-01	1.0018E 03	-6.5034E-01	8	11
2.40	8.8475E-01	1.2166E 03	-3.8673E-02	13	13
2.50	1.0010E 00	1.3028E 03	1.9851E-01	15	13
2.60	9.2021E-01	1.2488E 03	2.9679E-01	14	13
2.70	7.4740E-01	1.0967E 03	1.8031E-01	14	12
2.80	5.7750E-01	9.2042E 02	5.8553E-02	13	11
2.90	4.9668E-01	8.3395E 02	0.	11	10

TABLE II-2

COEFFICIENTS FOR INITIAL POSTBUCKLING BEHAVIOR OF BORON-EPOXY COMPOSITE CYLINDRICAL SHELLS

CASE	b	K	1/K	$\bar{\theta}$
1.00	-3.9794E-01	-1.4208E 00	-7.0384E-01	-1.0650E 02
1.10	-5.4781E-01	-2.1459E 00	-4.6601E-01	-1.1810E 02
1.20	-1.1065E 00	-4.3639E 00	-2.2915E-01	-1.2763E 02
1.30	-1.3955E 00	-8.1540E 00	-1.2264E-01	-1.3126E 02
1.40	-1.2528E 00	-1.0097E 01	-9.9043E-02	-1.3202E 02
1.50	-1.1986E 00	-6.9421E 00	-1.4405E-01	-1.3056E 02
1.60	-7.1149E-01	-5.0756E 00	-1.9702E-01	-1.2876E 02
1.70	-6.2618E-01	-2.5845E 00	-3.8693E-01	-1.2151E 02
1.80	-4.4361E-01	-1.2444E 00	-8.0357E-01	-1.0111E 02
1.90	-2.3891E-01	-4.7639E-01	-2.0991E 00	-4.2296E 01
2.00	-2.3434E-01	-3.6425E-01	-2.7453E 00	-2.9811E 01
2.10	-4.1941E-01	-7.3781E-01	-1.3554E 00	-7.0436E 01
2.20	-5.9229E-01	-9.5423E-01	-1.0480E 00	-8.7254E 01
2.30	-9.6021E-01	-1.9101E 00	-5.2354E-01	-1.1548E 02
2.40	-2.1958E 00	-4.7966E 00	-2.0848E-01	1.2836E 02
2.50	-1.9170E 00	-5.1617E 00	-1.9373E-01	-1.2888E 02
2.60	-1.7937E 00	-6.6479E 00	-1.5042E-01	-1.3035E 02
2.70	-1.1143E 00	-3.8724E 00	-2.5824E-01	-1.2657E 02
2.80	-5.9263E-01	-1.9795E 00	-5.0517E-01	-1.1633E 02
2.90	-3.9614E-01	-1.6518E 00	-6.0539E-01	-1.1153E 02

TABLE II-3

BUCKLING LOADS FOR IMPERFECT BORON-EPOXY SHELL
$\bar{w}^* = 0.01$

CASE	$\bar{N}_x$	$\bar{\bar{N}}_x$	ρ^*
1.0	4.6617E-01	7.8272E 02	9.3817E-01
1.10	5.2008E-01	8.5221E 02	9.3154E-01
1.20	6.6933E-01	1.0187E 03	9.1452E-01
1.30	8.4350E-01	1.1600E 03	9.0808E-01
1.40	9.1686E-01	1.1914E 03	9.1112E-01
1.50	8.3732E-01	1.1129E 03	9.1235E-01
1.60	6.9906E-01	1.0010E 03	9.2562E-01
1.70	5.5483E-01	8.8378E 02	9.2857E-01
1.80	4.2897E-01	7.8913E 02	9.3599E-01
1.90	3.6182E-01	7.3953E 02	9.4749E-01
2.0	3.4980E-01	7.4106E 02	9.4782E-01
2.10	3.5895E-01	7.3567E 02	9.3712E-01
2.20	4.2847E-01	7.9537E 02	9.2982E-01
2.30	5.7726E-01	9.1990E 02	9.1824E-01
2.40	7.9112E-01	1.0879E 03	8.9418E-01
2.50	8.9943E-01	1.1706E 03	8.9853E-01
2.60	8.2874E-01	1.1247E 03	9.0060E-01
2.70	6.8337E-01	1.0027E 03	9.1433E-01
2.80	5.3696E-01	8.5581E 02	9.2981E-01
2.90	4.6601E-01	7.8246E 02	9.3826E-01

TABLE II-4

BUCKLING LOADS FOR IMPERFECT BORON-EPOXY SHELL
$\bar{W}^* = 0.02$

CASE	$\bar{N}_x$	$\dot{\bar{N}}_x$	ρ^*
1. 0	4.4930E-01	7.5441E 02	9.0423E-01
1.10	4.9926E-01	8.1809E 02	8.9424E-01
1.20	6.3591E-01	9.6782E 02	8.6886E-01
1.30	7.9824E-01	1.0977E 03	8.5935E-01
1.40	8.6929E-01	1.1296E 03	8.6384E-01
1.50	7.9446E-01	1.0559E 03	8.6565E-01
1.60	6.6866E-01	9.5745E 02	8.8538E-01
1.70	5.3166E-01	8.4687E 02	8.8979E-01
1.80	4.1291E-01	7.5958E 02	9.0094E-01
1.90	3.5070E-01	7.1679E 02	9.1837E-01
2. 0	3.3911E-01	7.1842E 02	9.1886E-01
2.10	3.4575E-01	7.0861E 02	9.0265E-01
2.20	4.1089E-01	7.6273E 02	8.9167E-01
2.30	5.4969E-01	8.7596E 02	8.7438E-01
2.40	7.4230E-01	1.0207E 03	8.3900E-01
2.50	8.4619E-01	1.1013E 03	8.4535E-01
2.60	7.8069E-01	1.0595E 03	8.4838E-01
2.70	6.4918E-01	9.5257E 02	8.6858E-01
2.80	5.1493E-01	8.2069E 02	8.9165E-01
2.90	4.4918E-01	7.5419E 02	9.0436E-01

TABLE II-5

BUCKLING LOADS FOR IMPERFECT BORON-EPOXY SHELL
$\overline{W}^* = 0.04$

CASE	$\overline{N}_x$	$\dot{\overline{N}}_x$	ρ^*
1.0	4.2419E-01	7.1224E 02	8.5369E-01
1.10	4.6847E-01	7.6764E 02	8.3910E-01
1.20	5.8738E-01	8.9397E 02	8.0256E-01
1.30	7.3296E-01	1.0080E 03	7.8907E-01
1.40	8.0044E-01	1.0401E 03	7.9543E-01
1.50	7.3237E-01	9.7339E 02	7.9799E-01
1.60	6.2401E-01	8.9350E 02	8.2625E-01
1.70	4.9751E-01	7.9246E 02	8.3263E-01
1.80	3.8904E-01	7.1568E 02	8.4886E-01
1.90	3.3397E-01	6.8261E 02	8.7457E-01
2.0	3.2304E-01	6.8436E 02	8.7530E-01
2.10	3.2611E-01	6.6835E 02	8.5137E-01
2.20	3.8494E-01	7.1456E 02	8.3535E-01
2.30	5.0949E-01	8.1190E 02	8.1044E-01
2.40	6.7295E-01	9.2535E 02	7.6061E-01
2.50	7.7020E-01	1.0024E 03	7.6943E-01
2.60	7.1193E-01	9.6615E 02	7.7366E-01
2.70	5.9953E-01	8.7973E 02	8.0216E-01
2.80	4.8240E-01	7.6885E 02	8.3532E-01
2.90	4.2411E-01	7.1210E 02	8.5389E-01

TABLE II-6

BUCKLING LOADS FOR IMPERFECT BORON-EPOXY SHELL
$\overline{W}^* = 0.06$

CASE	$\overline{N}_x$	$\dot{\overline{N}}_x$	ρ^*
1. 0	4.0458E-01	6.7932E 02	8.1423E-01
1.10	4.4462E-01	7.2856E 02	7.9638E-01
1.20	5.5054E-01	8.3789E 02	7.5221E-01
1.30	6.8377E-01	9.4032E 02	7.3612E-01
1.40	7.4838E-01	9.7245E 02	7.4369E-01
1.50	6.8534E-01	9.1089E 02	7.4675E-01
1.60	5.8965E-01	8.4431E 02	7.8075E-01
1.70	4.7114E-01	7.5047E 02	7.8850E-01
1.80	3.7046E-01	6.8149E 02	8.0831E-01
1.90	3.2077E-01	6.5563E 02	8.4000E-01
2. 0	3.1035E-01	6.5747E 02	8.4091E-01
2.10	3.1079E-01	6.3696E 02	8.1139E-01
2.20	3.6487E-01	6.7731E 02	7.9181E-01
2.30	4.7883E-01	7.6305E 02	7.6167E-01
2.40	6.2153E-01	8.5465E 02	7.0249E-01
2.50	7.1358E-01	9.2872E 02	7.1287E-01
2.60	6.6058E-01	8.9645E 02	7.1785E-01
2.70	5.6185E-01	8.2443E 02	7.5174E-01
2.80	4.5725E-01	7.2877E 02	7.9178E-01
2.90	4.0453E-01	6.7923E 02	8.1447E-01

TABLE II-7

BUCKLING LOADS FOR IMPERFECT BORON-EPOXY SHELL
$W^* = 0.08$

CASE	$\overline{N}_x$	$\overset{o}{N}_x$	ρ^*
1.0	3.8812E-01	6.5168E 02	7.8110E-01
1.10	4.2472E-01	6.9596E 02	7.6074E-01
1.20	5.2031E-01	7.9189E 02	7.1092E-01
1.30	6.4368E-01	8.8518E 02	6.9295E-01
1.40	7.0581E-01	9.1711E 02	7.0140E-01
1.50	6.4685E-01	8.5973E 02	7.0481E-01
1.60	5.6116E-01	8.0351E 02	7.4303E-01
1.70	4.4921E-01	7.1554E 02	7.5180E-01
1.80	3.5489E-01	6.5285E 02	7.7434E-01
1.90	3.0958E-01	6.3276E 02	8.1070E-01
2.0	2.9959E-01	6.3468E 02	8.1175E-01
2.10	2.9795E-01	6.1064E 02	7.7785E-01
2.20	3.4817E-01	6.4630E 02	7.5555E-01
2.30	4.5359E-01	7.2282E 02	7.2153E-01
2.40	5.8019E-01	7.9780E 02	6.5575E-01
2.50	6.6785E-01	8.6921E 02	6.6719E-01
2.60	6.1902E-01	8.4006E 02	6.7269E-01
2.70	5.3094E-01	7.7908E 02	7.1038E-01
2.80	4.3631E-01	6.9539E 02	7.5552E-01
2.90	3.8810E-01	6.5163E 02	7.8138E-01

TABLE II-8

BUCKLING LOADS FOR IMPERFECT BORON-EPOXY SHELL
$W^* = 0.10$

CASE	$\overline{N}_x$	$\overset{\circ}{\overline{N}}_x$	ρ^*
1.0	3.7380E-01	6.2764E 02	7.5228E-01
1.10	4.0751E-01	6.6776E 02	7.2992E-01
1.20	4.9455E-01	7.5268E 02	6.7571E-01
1.30	6.0969E-01	8.3843E 02	6.5636E-01
1.40	6.6964E-01	8.7013E 02	6.6544E-01
1.50	6.1410E-01	8.1620E 02	6.6912E-01
1.60	5.3664E-01	7.6840E 02	7.1056E-01
1.70	4.3029E-01	6.8540E 02	7.2014E-01
1.80	3.4137E-01	6.2798E 02	7.4484E-01
1.90	2.9977E-01	6.1270E 02	7.8501E-01
2.0	2.9015E-01	6.1468E 02	7.8617E-01
2.10	2.8678E-01	5.8775E 02	7.4870E-01
2.20	3.3374E-01	6.1951E 02	7.2424E-01
2.30	4.3201E-01	6.8843E 02	6.8719E-01
2.40	5.4555E-01	7.5017E 02	6.1661E-01
2.50	6.2940E-01	8.1917E 02	6.2877E-01
2.60	5.8401E-01	7.9255E 02	6.3469E-01
2.70	5.0460E-01	7.4043E 02	6.7514E-01
2.80	4.1822E-01	6.6656E 02	7.2420E-01
2.90	3.7380E-01	6.2762E 02	7.5259E-01

TABLE II-9

BUCKLING LOADS FOR IMPERFECT BORON-EPOXY SHELL
$\overline{W}^* = 0.20$

CASE	$\overline{N}_x$	$\overset{\circ}{\overline{N}}_x$	ρ^*
1. 0	3.2053E-01	5.3819E 02	6.4508E-01
1.10	3.4436E-01	5.6427E 02	6.1680E-01
1.20	4.0313E-01	6.1354E 02	5.5080E-01
1.30	4.9055E-01	6.7460E 02	5.2811E-01
1.40	5.4210E-01	7.0441E 02	5.3870E-01
1.50	4.9837E-01	6.6238E 02	5.4302E-01
1.60	4.4771E-01	6.4107E 02	5.9282E-01
1.70	3.6127E-01	5.7546E 02	6.0462E-01
1.80	2.9130E-01	5.3587E 02	6.3560E-01
1.90	2.6256E-01	5.3666E 02	6.8757E-01
2. 0	2.5433E-01	5.3879E 02	6.8912E-01
2.10	2.4534E-01	5.0282E 02	6.4051E-01
2.20	2.8096E-01	5.2155E 02	6.0971E-01
2.30	3.5487E-01	5.6550E 02	5.6448E-01
2.40	4.2726E-01	5.8751E 02	4.8291E-01
2.50	4.9704E-01	6.4689E 02	4.9654E-01
2.60	4.6304E-01	6.2838E 02	5.0319E-01
2.70	4.1116E-01	6.0332E 02	5.5012E-01
2.80	3.5208E-01	5.6114E 02	6.0966E-01
2.90	3.2059E-01	5.3829E 02	6.4547E-01

TABLE II-10

BUCKLING LOADS FOR IMPERFECT BORON-EPOXY SHELL
$\overline{W}^* = 0.30$

CASE	$\overline{N_x}$	$\frac{\circ}{N_x}$	ρ^*
1. 0	2.8380E-01	4.7653E 02	5.7116E-01
1.10	3.0165E-01	4.9428E 02	5.4029E-01
1.20	3.4418E-01	5.2383E 02	4.7026E-01
1.30	4.1506E-01	5.7079E 02	4.4683E-01
1.40	4.6061E-01	5.9853E 02	4.5773E-01
1.50	4.2418E-01	5.6379E 02	4.6220E-01
1.60	3.8858E-01	5.5640E 02	5.1452E-01
1.70	3.1499E-01	5.0173E 02	5.2716E-01
1.80	2.5700E-01	4.7278E 02	5.6076E-01
1.90	2.3619E-01	4.8275E 02	6.1850E-01
2. 0	2.2891E-01	4.8494E 02	6.2024E-01
2.10	2.1686E-01	4.4444E 02	5.6614E-01
2.20	2.4545E-01	4.5562E 02	5.3264E-01
2.30	3.0461E-01	4.8542E 02	4.8454E-01
2.40	3.5496E-01	4.8810E 02	4.0120E-01
2.50	4.1523E-01	5.4042E 02	4.1482E-01
2.60	3.8787E-01	5.2637E 02	4.2150E-01
2.70	3.5095E-01	5.1496E 02	4.6955E-01
2.80	3.0757E-01	4.9020E 02	5.3259E-01
2.90	2.8390E-01	4.7668E 02	5.7159E-01

TABLE II-11

BUCKLING LOADS FOR IMPERFECT BORON-EPOXY SHELL
$\overline{W}^* = 0.40$

CASE	$\overline{N_x}$	$\dot{\overline{N}}_x$	ρ^*
1.00	2.5594E-01	4.2974E 02	5.1508E-01
1.10	2.6973E-01	4.4198E 02	4.8312E-01
1.20	3.0170E-01	4.5917E 02	4.1222E-01
1.30	3.6135E-01	4.9693E 02	3.8902E-01
1.40	4.0229E-01	5.2275E 02	3.9978E-01
1.50	3.7096E-01	4.9305E 02	4.0420E-01
1.60	3.4496E-01	4.9394E 02	4.5676E-01
1.70	2.8062E-01	4.4700E 02	4.6965E-01
1.80	2.3111E-01	4.2515E 02	5.0427E-01
1.90	2.1573E-01	4.4094E 02	5.6494E-01
2.00	2.0918E-01	4.4315E 02	5.6679E-01
2.10	1.9530E-01	4.0025E 02	5.0986E-01
2.20	2.1901E-01	4.0654E 02	4.7526E-01
2.30	2.6812E-01	4.2726E 02	4.2649E-01
2.40	3.0486E-01	4.1921E 02	3.4457E-01
2.50	3.5809E-01	4.6605E 02	3.5773E-01
2.60	3.3516E-01	4.5484E 02	3.6422E-01
2.70	3.0757E-01	4.5131E 02	4.1152E-01
2.80	2.7443E-01	4.3739E 02	4.7520E-01
2.90	2.5606E-01	4.2993E 02	5.1553E-01

TABLE II-12

BUCKLING LOADS FOR IMPERFECT BORON-EPOXY SHELL
$\overline{W}^* = 0.50$

CASE	$\overline{N_x}$	$\overset{\circ}{N}_x$	ρ^*
1. 0	2.3372E-01	3.9243E 02	4.7036E-01
1.10	2.4459E-01	4.0078E 02	4.3809E-01
1.20	2.6921E-01	4.0973E 02	3.6783E-01
1.30	3.2070E-01	4.4102E 02	3.4525E-01
1.40	3.5793E-01	4.6510E 02	3.5569E-01
1.50	3.3040E-01	4.3913E 02	3.6000E-01
1.60	3.1097E-01	4.4527E 02	4.1175E-01
1.70	2.5370E-01	4.0412E 02	4.2460E-01
1.80	2.1055E-01	3.8732E 02	4.5940E-01
1.90	1.9912E-01	4.0698E 02	5.2142E-01
2. 0	1.9314E-01	4.0917E 02	5.2333E-01
2.10	1.7814E-01	3.6509E 02	4.6506E-01
2.20	1.9825E-01	3.6800E 02	4.3021E-01
2.30	2.4004E-01	3.8251E 02	3.8182E-01
2.40	2.6770E-01	3.6811E 02	3.0257E-01
2.50	3.1544E-01	4.1055E 02	3.1513E-01
2.60	2.9571E-01	4.0130E 02	3.2135E-01
2.70	2.7440E-01	4.0265E 02	3.6714E-01
2.80	2.4841E-01	3.9592E 02	4.3015E-01
2.90	2.3385E-01	3.9264E 02	4.7082E-01

TABLE II-13

BUCKLING LOADS FOR IMPERFECT BORON-EPOXY SHELL
$\overline{W}^* = 0.80$

CASE	$\overline{N}_x$	$\overset{\circ}{\overline{N}}_x$	ρ^*
1. 0	1.8682E-01	3.1368E 02	3.7597E-01
1.10	1.9249E-01	3.1541E 02	3.4477E-01
1.20	2.0467E-01	3.1149E 02	2.7964E-01
1.30	2.4106E-01	3.3151E 02	2.5952E-01
1.40	2.7047E-01	3.5145E 02	2.6878E-01
1.50	2.5020E-01	3.3254E 02	2.7262E-01
1.60	2.4160E-01	3.4595E 02	3.1991E-01
1.70	1.9836E-01	3.1596E 02	3.3197E-01
1.80	1.6741E-01	3.0797E 02	3.6528E-01
1.90	1.6305E-01	3.3326E 02	4.2697E-01
2. 0	1.5830E-01	3.3536E 02	4.2892E-01
2.10	1.4203E-01	2.9108E 02	3.7079E-01
2.20	1.5542E-01	2.8851E 02	3.3728E-01
2.30	1.8376E-01	2.9283E 02	2.9231E-01
2.40	1.9691E-01	2.7077E 02	2.2257E-01
2.50	2.3352E-01	3.0393E 02	2.3329E-01
2.60	2.1961E-01	2.9803E 02	2.3865E-01
2.70	2.0854E-01	3.0600E 02	2.7902E-01
2.80	1.9475E-01	3.1039E 02	3.3722E-01
2.90	1.8696E-01	3.1392E 02	3.7642E-01

TABLE II-14

BUCKLING LOADS FOR IMPERFECT BORON-EPOXY SHELL
$\overline{W}^* = 0.90$

CASE	$\overline{N}_x$	$\overset{\circ}{N}_x$	ρ^*
1.0	1.7535E-01	2.9443E 02	3.5290E-01
1.10	1.7996E-01	2.9489E 02	3.2234E-01
1.20	1.8972E-01	2.8874E 02	2.5922E-01
1.30	2.2285E-01	3.0646E 02	2.3991E-01
1.40	2.5035E-01	3.2530E 02	2.4878E-01
1.50	2.3171E-01	3.0796E 02	2.5247E-01
1.60	2.2516E-01	3.2240E 02	2.9813E-01
1.70	1.8514E-01	2.9491E 02	3.0986E-01
1.80	1.5693E-01	2.8868E 02	3.4241E-01
1.90	1.5401E-01	3.1478E 02	4.0330E-01
2.0	1.4955E-01	3.1663E 02	4.0523E-01
2.10	1.3323E-01	2.7304E 02	3.4781E-01
2.20	1.4517E-01	2.6947E 02	3.1503E-01
2.30	1.7063E-01	2.7191E 02	2.7142E-01
2.40	1.8110E-01	2.4903E 02	2.0470E-01
2.50	2.1510E-01	2.7995E 02	2.1488E-01
2.60	2.0243E-01	2.7471E 02	2.1998E-01
2.70	1.9329E-01	2.8363E 02	2.5862E-01
2.80	1.8190E-01	2.8991E 02	3.1497E-01
2.90	1.7550E-01	2.9467E 02	3.5334E-01

TABLE II-15

BUCKLING LOADS FOR IMPERFECT BORON-EPOXY SHELL
$\overline{w}^* = 1.00$

CASE	$\overline{N}_x$	$\dot{\overline{N}}_x$	ρ^*
1. 0	1.6529E-01	2.7753E 02	3.3264E-01
1.10	1.6903E-01	2.7698E 02	3.0276E-01
1.20	1.7686E-01	2.6917E 02	2.4165E-01
1.30	2.0725E-01	2.8500E 02	2.2311E-01
1.40	2.3308E-01	3.0286E 02	2.3162E-01
1.50	2.1582E-01	2.8685E 02	2.3516E-01
1.60	2.1088E-01	3.0196E 02	2.7923E-01
1.70	1.7365E-01	2.7660E 02	2.9062E-01
1.80	1.4774E-01	2.7178E 02	3.2236E-01
1.90	1.4599E-01	2.9839E 02	3.8230E-01
2. 0	1.4180E-01	3.0040E 02	3.8421E-01
2.10	1.2551E-01	2.5722E 02	3.2766E-01
2.20	1.3624E-01	2.5289E 02	2.9564E-01
2.30	1.5930E-01	2.5385E 02	2.5340E-01
2.40	1.6768E-01	2.3057E 02	1.8952E-01
2.50	1.9941E-01	2.5953E 02	1.9921E-01
2.60	1.8779E-01	2.5485E 02	2.0407E-01
2.70	1.8010E-01	2.6438E 02	2.4107E-01
2.80	1.7070E-01	2.7207E 02	2.9559E-01
2.90	1.6543E-01	2.7777E 02	3.3307E-01

TABLE II-16

BUCKLING LOADS FOR IMPERFECT BORON-EPOXY SHELL
$\overline{W}^* = 1.10$

CASE	$\bar{N}_x$	$\dot{\bar{N}}_x$	ρ^*
1. 0	1.5637E-01	2.6255E 02	3.1469E-01
1.10	1.5940E-01	2.6120E 02	2.8552E-01
1.20	1.6567E-01	2.5214E 02	2.2636E-01
1.30	1.9372E-01	2.6641E 02	2.0856E-01
1.40	2.1808E-01	2.8338E 02	2.1672E-01
1.50	2.0202E-01	2.6850E 02	2.2012E-01
1.60	1.9836E-01	2.8403E 02	2.6265E-01
1.70	1.6354E-01	2.6050E 02	2.7370E-01
1.80	1.3962E-01	2.5684E 02	3.0463E-01
1.90	1.3882E-01	2.8373E 02	3.6351E-01
2. 0	1.3486E-01	2.8570E 02	3.6541E-01
2.10	1.1867E-01	2.4321E 02	3.0981E-01
2.20	1.2838E-01	2.3830E 02	2.7859E-01
2.30	1.4942E-01	2.3810E 02	2.3767E-01
2.40	1.5613E-01	2.1470E 02	1.7647E-01
2.50	1.8589E-01	2.4193E 02	1.8570E-01
2.60	1.7515E-01	2.3770E 02	1.9034E-01
2.70	1.6877E-01	2.4764E 02	2.2580E-01
2.80	1.6086E-01	2.5637E 02	2.7854E-01
2.90	1.5651E-01	2.6279E 02	3.1511E-01

TABLE II-17

BUCKLING LOADS FOR IMPERFECT BORON-EPOXY SHELL
$\overline{W}^* = 1.20$

CASE	$\overline{N}_x$	$\dot{\overline{N}}_x$	ρ^*
1.00	1.4840E-01	2.4917E 02	2.9865E-01
1.10	1.5085E-01	2.4718E 02	2.7019E-01
1.20	1.5583E-01	2.3717E 02	2.1292E-01
1.30	1.8189E-01	2.5013E 02	1.9581E-01
1.40	2.0493E-01	2.6629E 02	2.0365E-01
1.50	1.8990E-01	2.5240E 02	2.0692E-01
1.60	1.8728E-01	2.6817E 02	2.4798E-01
1.70	1.5458E-01	2.4622E 02	2.5870E-01
1.80	1.3237E-01	2.4351E 02	2.8882E-01
1.90	1.3235E-01	2.7052E 02	3.4660E-01
2.00	1.2860E-01	2.7245E 02	3.4846E-01
2.10	1.1257E-01	2.3070E 02	2.9388E-01
2.20	1.2140E-01	2.2536E 02	2.6345E-01
2.30	1.4071E-01	2.2423E 02	2.2383E-01
2.40	1.4609E-01	2.0089E 02	1.6512E-01
2.50	1.7411E-01	2.2660E 02	1.7393E-01
2.60	1.6413E-01	2.2274E 02	1.7837E-01
2.70	1.5874E-01	2.3293E 02	2.1239E-01
2.80	1.5212E-01	2.4244E 02	2.6340E-01
2.90	1.4854E-01	2.4940E 02	2.9906E-01

REFERENCES

1. Koiter, W. T., "Elastic Stability and Post-Buckling Behavior," in Nonlinear Problems, edited by Langer, R. E., University of Wisconsin Press, Madison, Wisconsin (1963).

2. Koiter, W. T., "On the Stability of Elastic Equilibrium," Ph.D. Thesis, Delft, Amsterdam (1945), (Translation as AFFDL-TR-70-25).

3. Koiter, W. T., "The Stability of Elastic Systems," NASA TT F-10, 833.

4. Budianski, B., and J. W. Hutchinson, "Dynamic Buckling of Imperfection Sensitive Structures," Proceedings of the XI International Congress of Appl. Mech., edited by H. Gortler, Springer-Verlag (1964).

5. Budianski, B., "Dynamic Buckling of Elastic Structures Criteria and Estimates," Proceedings International Conference on Dynamic Stability of Structures, Pergamon Press, New York (1966).

6. Budianski, B., "Post Buckling Behavior of Cylinders in Torsion," Second IUTAM Proceedings on Thin Shells, Copenhagen, Aug. 1964.

7. Koiter, W. T., "The Effect of Axisymmetric Imperfections on the Buckling of Cylindrical Shells under Axial Compression," Koninkl. Ned. Akad. Weterschap. Proc., B66, 265 (1963).

8. Budianski, B., and J. C. Amazigo, "Initial Post-Buckling Behavior of Cylindrical Shells under External Pressure," J. Math and Phys., 47, 223-235 (1968).

9. Hutchinson, J. W., "Initial Post-Buckling Behavior of Toroidal Shell Segments," Int. J. Solids Structures, 3, 97-115 (1967).

10. Hutchinson, J. W., and J. C. Amazigo, "Imperfection Sensitivity of Eccentrically Stiffened Cylindrical Shells," AIAA J., 5, 392-401 (1967).

11. Hutchinson, J. W., "Imperfection Sensitivity of Externally Pressurized Spherical Shells," J. Appl. Mech., 3, 49-55 (1967).

12. Hutchinson, J. W., "Buckling and Initial Post-Buckling Behavior of Oval Cylindrical Shells under Axial Compression," J. Appl. Mech., 3, 66-72 (1968).

13. Hutchinson, J. W., "Axial Buckling of Pressurized Imperfect Cylindrical Shells," AIAA J., 3, 1461-1466 (1965).

14. Hutchinson, J. W., and J. C. Frauenthal, "Elastic Post-Buckling Behavior of Stiffened and Barreled Cylindrical Shells," J. Applied Mech., 12, 784-790 (1969).

15. Fitch, J. R., "The Buckling and Post-Buckling Behavior of Spherical Caps Under Concentrated Load," Int. J. Solids Structures, 4, 421-446 (1968).

REFERENCES (CONTD)

16. Hutchinson, J. W., "Buckling of Imperfect Cylindrical Shells under Axial Compression and External Pressure," AIAA J., 3, 1968-1970 (1968).

17. Budiansky, B., and J. M. Hutchinson, "A Survey of Some Buc'ling Problems," AIAA J., 4, 1505-1510 (1966).

18. Amazigo, J. C., "Buckling under Axial Compression of Long Cylindrical Shells with Random Axisymmetric Imperfections," Quart. Appl. Math., 26, 537-566 (1969).

19. Hutchinson, J. W., R. C. Tennyson, and D. B. Muggeridge, "The Effect of a Local Axisymmetric Imperfection on the Buckling Behavior of a Circular Cylindrical Shell under Axial Compression," presented at AIAA 8th Aerospace Sciences Meeting, New York, Jan 19-21, 1970 (70-103).

20. Tennyson, R. C., and D. B. Muggeridge, "Buckling of Axisymmetric Imperfect Circular Cylindrical Shells under Axial Compression, AIAA J., 7, 2127 (1969).

21. Arbocz, J., and C. D. Babcock, "The Effect of General Imperfections on the Buckling of Cylindrical Shells," J. Appl. Mech., 3, 28-38 (1969).

22. Brush, D. O., "Imperfection Sensitivity of Stringer Stiffened Cylinders," AIAA J., 6, 2445-2446 (1968).

23. Ambartsumyan, S. A., "Theory of Anisotropic Shells," NASA-TTF-118 (1964).

24. Dong, S. B., K. S. Pister, and R. L. Taylor, "On the Theory of Laminated Anisotropic Shells and Plates," J. Aero. Sci., Vol. 29, No. 8, 969 (1962).

25. Cheng, S., and B. P. C. Ho, "Stability of Heterogeneous Aerolotropic Cylindrical Shells under Combined Loading," AIAA J., 1, 1603 (1963).

26. Holston, Jr., A., A. Feldman, and D. A. Stang, Stability of Filament Wound Cylinders under Combined Loading, AFFDL-TR-67-55 Air Force Flight Dynamics Laboratory, Wright-Patterson Air Force Base, Ohio (1967).

27. Tasi, J., A. Feldman, and D. A. Stang, "The Buckling Strength of Filament-Wound Cylinders Under Axial Compression," NASA-CR-266 (1965).

28. Khot, N. S., "Buckling and Post-Buckling Behavior of Composite Cylindrical Shells under Axial Compression," AIAA J., 2, 229-235 (1970).

29. Khot, N. S., "Post-Buckling Behavior of Geometrically Imperfect Composite Cylindrical Shells Under Axial Compression," AIAA J., 3, 579-581 (1970).

REFERENCES (CONTD)

30. Khot, N. S., V. B. Venkayya, and L. Berke, "Buckling and Postbuckling Behavior of Initially Imperfect Orthotropic Cylindrical Shells Under Axial Compression and Internal Pressure," presented at IUTAM Conference on Instability of Continuous Systems held at Herrenalb, West Germany, Sep 8-12, 1969.

31. Khot, N.S., On the Effects of Fiber Orientation and Nonhomogeneity on Buckling and Postbuckling Behavior of Fiber-Reinforced Cylindrical Shells under Axial Compression, AFFDL-TR-68-19 Air Force Flight Dynamics Laboratory, Wright-Patterson Air Force Base, Ohio (1968).

32. Khot, N.S., On the Influence of Initial Geometric Imperfections on the Buckling and Postbuckling Behavior of Fiber-Reinforced Cylindrical Shells under Uniform Axial Compression, AFFDL-TR-68-136 Air Force Flight Dynamics Laboratory, Wright-Patterson Air Force Base, Ohio (1968).

UNCLASSIFIED

Security Classification

DOCUMENT CONTROL DATA - R & D

(Security classification of title, body of abstract and indexing annotation must be entered when the overall report is classified)

1. ORIGINATING ACTIVITY (Corporate author) Air Force Flight Dynamics Laboratory Wright-Patterson Air Force Base, Ohio 45433	2a. REPORT SECURITY CLASSIFICATION UNCLASSIFIED 2b. GROUP

3. REPORT TITLE

EFFECT OF FIBER ORIENTATION ON INITIAL POSTBUCKLING BEHAVIOR AND IMPERFECTION SENSITIVITY OF COMPOSITE CYLINDRICAL SHELLS

4. DESCRIPTIVE NOTES (Type of report and inclusive dates)

December 1969 to May 1970

5. AUTHOR(S) (First name, middle initial, last name)

N. S. Khot
V. B. Venkayya

6. REPORT DATE	7a. TOTAL NO. OF PAGES	7b. NO. OF REFS
December 1970	86	32

8a. CONTRACT OR GRANT NO.	9a. ORIGINATOR'S REPORT NUMBER(S)
b. PROJECT NO. 1467	AFFDL-TR-70-125
c. Task No. 146703	9b. OTHER REPORT NO(S) (Any other numbers that may be assigned this report)
d. Work Unit 146703-010	

10. DISTRIBUTION STATEMENT

This document has been approved for public release and sale; its distribution is unlimited.

11. SUPPLEMENTARY NOTES	12. SPONSORING MILITARY ACTIVITY
	Air Force Flight Dynamics Laboratory Wright-Patterson AFB, Ohio 45433

13. ABSTRACT

Koiter's approach is used to formulate the influence of fiber orientation on the behavior of the cylindrical shell in the initial postbuckling region. Results are presented for three-layer composite cylindrical shells of either glass-epoxy or boron-epoxy subjected to uniform axial compressive load. The results show that the initial postbuckling coefficient that characterizes the extent of imperfection sensitivity of a structure is greater for the glass-epoxy shells than for the boron-epoxy shells. For the glass-epoxy cylinders the slope of the load vs. end-shortening curve in the initial postbuckling region is found to have high negative value, which is not significantly affected by the change in fiber orientation. This suggests that the buckling of a nearly perfect glass-epoxy cylinder under prescribed end-shortening will be catastrophic, regardless of fiber orientation. However, for the boron-epoxy cylinders the negative slope varies with the change in fiber orientation, and whether the failure will be catastrophic or not will depend on the fiber orientation.

DD FORM 1 NOV 65 1473

UNCLASSIFIED

Security Classification

14. KEY WORDS	LINK A		LINK B		LINK C	
	ROLE	WT	ROLE	WT	ROLE	WT
Buckling						
Composites						
Fiber-Reinforced Material						
Circular Cylinders						
Axial Load						
Initial Postbuckling						
Imperfection Sensitivity						